ACTOMYOSIN SPATIOTEMPORALLY REGULATES PAR POLARITY DYNAMICS TO CREATE NEURAL STEM CELL ASYMMETRY

by

CHET HUAN OON

A DISSERTATION

Presented to the Department of Biology
and the Division of Graduate Studies of the University of Oregon
in partial fulfillment of the requirements
for the degree of
Doctor of Philosophy

June 2021

DISSERTATION APPROVAL PAGE

Student: Chet Huan Oon

Title: Actomyosin Spatiotemporally Regulates Par Polarity Dynamics to Create Neural Stem Cell Asymmetry

This dissertation has been accepted and approved in partial fulfillment of the requirements for the Doctor of Philosophy degree in the Department of Biology by:

Kryn Stankunas	Chairperson
Ken Prehoda	Advisor
Bruce Bowerman	Core Member
Tory Herman	Core Member
Brad Nolen	Core Member
Carrie McCurdy	Institutional Representative

and

Andy Karduna	Interim Vice Provost for Graduate Studies

Original approval signatures are on file with the University of Oregon Division of Graduate Studies.

Degree awarded June 2021

DISSERTATION ABSTRACT

Chet Huan Oon

Doctor of Philosophy

Department of Biology

June 2021

Title: Actomyosin Spatiotemporally Regulates Par Polarity Dynamics to Create Neural Stem Cell Asymmetry

Pattern formation, or specifically symmetry breaking, is a fundamental process essential for proper asymmetric cell division. In asymmetrically dividing stem cells, the evolutionarily conserved Par polarity complex localizes to a discrete Par domain to facilitate unequal distribution of fate determinants into the daughter cells–thereby ensuring a binary cell division outcome where daughters will acquire distinct fates. Hence proper asymmetric cell division requires the spatiotemporal distribution of Par proteins to be precisely coordinated. While a number of studies have been conducted to understand how Par activity creates downstream asymmetry, how the Par complex acquires asymmetry remains unclear.

Two standing models exist to explain for how Par proteins can become polarized. In the one-cell stage *C. elegans* embryo, gradients of contractile force created by the cortical actomyosin cytoskeletal network generates cortical flow towards the anterior pole. Concurrently, symmetrical Par proteins that are entrained within the network becomes advected via bulk motion of the cortex, consequently becoming anteriorly segregated. In *Drosophila* neuroblasts, Par complex exchanges between the unpolarized,

cytoplasmic and polarized, apical states; it is thus thought to become polarized to the apical domain via a direct, asymmetric targeting mechanism.

In this dissertation, we examined the spatiotemporal distribution profile of cortical Par proteins and actomyosin in mitotic neuroblasts using a full volume, rapid live imaging approach to capture change in cortical protein distribution as they transition from an unpolarized to a polarized state. In the second chapter, we characterized the Par protein dynamics and investigated if the actomyosin network is essential for Par dynamics. This study demonstrated that Par polarization is a dynamic, multistep process, consisting of asymmetric targeting of cytoplasmic Par into discrete, apical foci and F-actin dependent coalescence of Par foci at the apical pole. In the third chapter, we determined the cortical dynamics of actomyosin and identified that coalescence is spatiotemporally linked to myosin II driven flow. Our studies suggest a conserved role for actomyosin in Par polarity in *C. elegans* embryos and *Drosophila* neuroblasts.

This dissertation contains previously published and unpublished co-authored material. Live imaging movies of Par proteins and actomyosin are attached in the supplemental files associated with this dissertation.

CURRICULUM VITAE

NAME OF AUTHOR: Chet Huan Oon

GRADUATE AND UNDERGRADUATE SCHOOLS ATTENDED:

University of Oregon, Eugene, OR
University of California San Diego, La Jolla, CA

DEGREES AWARDED:

Doctor of Philosophy, Biology, 2021, University of Oregon
Bachelor of Science, Biochemistry and Chemistry, 2015, University of California San Diego

AREAS OF SPECIAL INTEREST:

Molecular Biology
Cell Biology
Genetics

PROFESSIONAL EXPERIENCE:

Graduate Teaching Fellow, Department of Biology, University of Oregon, Eugene, Oregon, 2016-2017

Undergraduate Research Intern, Laboratories of Dr. Karl Willet and Dr. David Traver, University of California San Diego, La Jolla, CA, 2014-2016

GRANTS, AWARDS, AND HONORS:

Pete von Hippel Graduate Scholar Award, University of Oregon, 2020

College of Arts and Sciences (CAS) and Office of Vice President for Research and Innovation (OVPRI) Genetics Training Grant Appointee, University of Oregon, 2017-2019

Stanley David and Lucille Borgen Adamson Memorial Scholarship Award, University of Oregon, 2016

PUBLICATIONS:

Oon, C. H. & Prehoda, K. E. 2021. Phases of actomyosin contractions underlie Par polarity during the neuroblast polarity cycle. *eLife*, *manuscript under revision.*

Oon, C. H. & Prehoda, K. E. (2019). Asymmetric recruitment and actin dependent cortical flows drive the neuroblast polarity cycle. *eLife* **8**. doi: 10.7554/eLife.45815

Grainger, S., Nguyen, N., Richter, J., Setayesh, J., Lonquich, B., **Oon, C. H**, Wozniak, J., Barahona, R., Kamei, C., Houston, J., Carrilo-Terrazas, M., Drummond, I., Gonzalez, D., Willert, K., Traver, D. 2019. EGFR is required for Wnt9a/Fzd9b signaling specificity in haematopoietic stem cells. *Nat Cell Biol* **21**:721-730. doi: 10.1038/s41556-019-0330-5

Grainger, S., Lonquich, B., **Oon, C. H**, Nguyen, N. Willert, K., Traver, D. 2017. CRISPR Guide RNA Validation In Vitro. *Zebrafish* **14**:383-386. doi:10.1089/zeb.2016.1358

ACKNOWLEDGMENTS

First, I would like to thank my advisor, Dr. Ken Prehoda, for his unwavering support throughout my graduate training. Throughout the years, he has spent numerous hours patiently transferring his knowledge, wisdom, and scientific philosophy to me and has given me countless opportunities and room to experiment, fail, and begin again. I am tremendously grateful to have his guidance over the years and to have him as my graduate mentor. I have also been very fortunate to have the support of my committee members: Dr. Kryn Stankunas, Dr. Bruce Bowerman, Dr. Tory Herman, Dr. Brad Nolen, and Dr. Carrie McCurdy. Despite their busy schedule, they always found time to meet with me, attend my talks, offer insightful advice, and provide new perspective to approach my scientific questions. I would also like to thank my past and present Prehoda lab mates. Particularly, Dr. Matthew Bailey and Dr. Kimberly Jones were always there to provide any help or advice I needed and were incredibly supportive of my scientific endeavors. Others, including Dr. Ryan Holly, Nicole Paterson, Dr. Bryce LaFoya, Elizabeth Vargas, and Dr. Rhiannon Penkert were wonderful colleagues to work alongside. I would not have embarked on this journey had I not met Dr. Stephanie Grainger in the lab of Dr. Karl Willert. She taught me the basics I know before graduate school, gave me plenty of professional development advice, and made me believe in myself. I will be forever grateful to her for her mentorship and encouragement as well as for being an amazing role model. I am also incredibly thankful for Dr. Willert, who had given me the opportunity to start out as a young, budding scientist in his lab.

Finally, I would like to thank my family for their unconditional love and support. Thank you for all that I have and for believing in me.

To my family,

TABLE OF CONTENTS

Chapter Page

Chapter Page

LIST OF FIGURES

Figure Page

CHAPTER I

CELL POLARITY IN ASYMMETRICALLY DIVIDING STEM CELLS

^ This chapter contains unpublished co-authored material.

C.H. Oon and K.E. Prehoda

Institute of Molecular Biology, Department of Chemistry and Biochemistry

1229 University of Oregon, Eugene OR 97403

Author Contributions: C.H. Oon contributed to Conceptualization, Writing—original draft, Writing—review and editing. K.E. Prehoda contributed to Conceptualization, Writing—original draft, Writing—review and editing.

INTRODUCTION

Brief history of intrinsic asymmetric cell division

Our understanding of intrinsically induced asymmetric cell division was mainly derived from pioneering works done in invertebrate model systems, including: *C. elegans* embryos, *Drosophila* sensory organ precursors (SOP), and *Drosophila* neuroblasts. During the earlier stages of *C. elegans* embryogenesis, cytoplasmic factors such as intestinal differentiation marker and germline-specific P-granules become exclusively inherited into cells committed to the gut or the germline lineage, respectively (Laufer *et al.*, 1980; Strome & Wood, 1982). This lineage-specific inheritance of cytoplasmic

factors provided evidence supporting the preexisting hypothesis that factors outside of the nucleus can determine cell fate. Furthermore, isolated blastomere retains the ability to asymmetrically partition P-granules, suggesting that preferential segregation of these germ granules occurs cell-autonomously (Strome & Wood, 1982). These early observations, along with a number of other earlier studies, led to the speculation that cell fate determination can occur cell-intrinsically.

Thereafter genetic analysis identified one of the first known cell-intrinsic fate-determining cues in asymmetrically-dividing *Drosophila* SOPs and neuroblasts. SOP-cell expressing loss-of-function of *numb* allele divides symmetrically and fails to give rise to daughter cells of distinct fates (Uemura *et al.*, 1989). Subsequently, Numb, a Notch signaling inhibitor, and a number of other fate determining proteins were reported to localize asymmetrically to the cell cortex in a cell-cycle dependent manner to confer distinct fates to the progenies (Rhyu *et al.*, 1994; Hirata *et al.*, 1995; Knoblich *et al.*, 1995; Ikeshima-Kataoka *et al.*, 1997; Broadus & Doe, 1997; Schuldt *et al.*, 1998; Shen *et al.*, 1998; Betschinger *et al.*, 2006; Lee *et al.*, 2006; Bello *et al.*, 2006).

Upstream regulatory factors responsible for asymmetric segregation of these fate determination factors were reported at around a similar period. Genetic screen in *C. elegans* embryos identified several partitioning-defective (*par*) genes essential for mitotic spindle positioning and asymmetric partitioning of fate-determining proteins and RNAs in early development of the organism (Kemphues *et al.*, 1988). Of the six *par* genes initially identified, Par-3 and Par-6, along with atypical protein kinase C (aPKC)–the seventh member of the Par family (Tabuse *et al.*, 1998)–were found to assume

evolutionarily conserved roles in asymmetric cell division. Collectively, these three core members associate with one another to form the ternary Par polarity complex.

Par complex ensures proper asymmetric cell division

During asymmetric cell division, the Par complex localizes to a discrete, cortical Par domain to specify a polarity axis (Wodarz *et* al., 2000; Petronczki and Knoblich, 2001)–according to which they mediate mitotic spindle orientation, cell size asymmetry, and polarization of downstream Par substrates such as cortical fate determining proteins (Kuchinke *et* al*.,* 1998; Schober *et al.*, 1999; Cai *et* al., 2003; Rolls *et* al., 2003; Betschinger and Knoblich, 2004). These precisely coordinated processes ensure a binary cell division outcome, whereby daughter cells will inherit distinct cell fates following cytokinesis to enable generation of cell diversity (Venkei & Yamashita, 2018). For instance in larval *Drosophila* neuroblasts, mitotic spindles align in a paralleled manner to the pre-established polarity axis to ensure unequal cell size and biased segregation of differentiation factors to the progenies.

Upon being exclusively segregated into the differentiating daughter of the asymmetrically-dividing neuroblast, fate determinant and coiled-coil adaptor protein Miranda (Mira) begins to degrade, thereby releasing its cargoes–including transcriptional repressor Prospero (Pros; Hirata *et al.*, 1995; Knoblich *et al.*, 1995; Ikeshima-Kataoka *et al.*, 1997; Shen *et al.*, 1997; Schuldt *et al.*, 1998) and translational repressors Staufen (Stau; Broadus & Doe, 1997; Schuldt *et al.*, 1998; Shen *et al.*, 1998) and Brain tumor (Brat; Betschinger *et al.*, 2006; Lee *et al.*, 2006; Bello *et al.*, 2006)–from the cell cortex. Following cortical release, fate determinants translocate into the nucleus of the differentiating cell, where they can regulate cell proliferation and cell cycle progression,

as well as promote neuronal differentiation (Li & Vaessin, 2000; Choksi *et al.*, 2006; Betschinger *et al.*, 2006). Hence, proper asymmetric cell division requires the subcellular localization of fate determinants to be tightly regulated.

Fate determining proteins consist of a basic, hydrophobic motif that facilitates cortical association by interacting with membrane phospholipids. aPKC, a key member of the Par complex, phosphorylates this membrane binding motif, thereby causing a change in its electrostatic character and cortical release of the respective protein (Smith *et* al., 2007; Atwood and Prehoda, 2009; Bailey and Prehoda, 2015). Since aPKC activity is restricted to the Par domain, aPKC-mediated phosphoregulation can effectively partition fate determinants to the opposite domain in order to polarize them. This mode of polarization has also been reported as a key function of the Par complex in *C. elegans* embryos (Hurov *et al.*, 2004; Hao *et al.*, 2006; Beatty *et al.*, 2010; Motegi *et al.*, 2011).

CURRENT MODELS FOR PAR POLARIZATION

Despite its conserved roles in establishing spatial asymmetry and coordinating division orientation in *C. elegans*, *Drosophila*, *Xenopus*, and mammals (Doe & Bowerman, 2001), asymmetric organization of the Par complex is thought to occur via distinct, non-conserved mechanisms. Earlier studies from one-cell stage *C. elegans* embryos have shown that polarization of the Par complex is a highly dynamic process that is driven by the contractile cortical actomyosin network (Cheeks *et al.*, 2004; Munro *et al.*, 2004; Mayer *et al.*, 2010); while in *Drosophila* neuroblasts, preferential segregation of Par-3 (also known as Bazooka, or Baz, in neuroblasts) was reported to occur independently of non-muscle myosin II (hereafter myosin II; Barros *et al.*, 2003). Although no supporting data had been published on Par polarization in larval neuroblasts,

the Par complex was initially thought to directly target from the cytoplasm to its cortical Par domain via a one-step, asymmetric targeting mechanism. However, recent reexamination of the Par complex and actomyosin dynamics in larval neuroblasts suggests that the two well-established polarity models are likely utilizing similar actomyosin-driven mechanisms to polarize Par complex. Here in the following chapters, we describe how actomyosin functions dynamically to generate cortical asymmetry in the two polarity models–with greater emphasis on *Drosophila* neuroblasts–as well as identify unifying principles–where the two systems converge.

Actomyosin segregates Par complex via cortical flow in *C. elegans* embryos

Upon fertilization and meiosis completion, the one-cell stage *C. elegans* embryo (P_0) divides asymmetrically along the anterior-posterior (A-P) axis to generate a larger anterior blastomere (AB) and a smaller posterior P_1 blastomere. This first P_0 division determines AB progenies to be of the ectodermal lineage and P_1 progenies to be either from the mesodermal, endodermal, or germline lineage (Doe & Bowerman, 2001). After meiotic exit, the cortical meshwork composed of bundled actin filaments–crosslinked by dense myosin II foci–undergoes cycles of contraction and relaxation (Munro *et al.*, 2004). These contractile pulses lead to accumulation of the actin cytoskeleton and formation of cortical ruffles. At this stage prior to polarization, the actomyosin network is uniformly distributed and evenly tensioned across the worm embryo. Accordingly, the Par complex is symmetrically cortical at this time.

At around 30 minutes post-fertilization, appearance of the sperm pronucleus and its associated centrosome at the future posterior pole cue for symmetry breaking. Cortical actomyosin network proximal to the paternal centrosome weakens until contractility

ceases at the posterior pole. This non-contractile domain expands from the posterior toward the center of the nascent A-P axis. Meanwhile, as contraction continues in the rest of the cortex, the contractile cortex flows away from posterior and towards the anterior pole. Given that the Par complex is embedded within the cortical layer and that other cortical proteins not involved in polarity such as E-cadherin were also subjected to cortical flow, it is thought that cortical flow acts through passive advection to polarize the Par complex to the anterior pole. With anterior Par proteins vacated from the posterior pole, cytoplasmic Par-1 and Par-2 are loaded from the cytoplasm to the posterior cortex. Following establishment of Par polarity, mutual inhibition of the anterior and posterior Par proteins keeps them from reverting back to being unpolarized (Etemad-Moghadam *et al.*, 1995; Tabuse *et al.*, 1998; Cuenca *et al.*, 2003).

Asymmetric targeting facilitates Par polarization in *Drosophila* neuroblasts

In order to populate the developing *Drosophila* central nervous system, neuroblasts divides asymmetrically along the apical-basal (A-B) axis to generate a larger apical stem daughter and a smaller basal ganglion mother cell (GMC). In this asymmetric cell division, the apical daughter helps maintain the stem cell pool while the GMC gives rise to neurons and glia (Doe & Bowerman, 2001). During each round of division, neuroblasts establish polarity *de novo*. Initially unpolarized, cytoplasmic Par complex becomes targeted to a bright crescent at the apical cortex by metaphase (Wodarz *et* al., 2000; Petronczki & Knoblich, 2001). Post-cytokinesis, Par complex returns to its cytoplasmic distribution as this distribution pattern is repeated for each consecutive cycle of cell division. Unlike *C.* elegans embryos, polarization of Par complex was thought to be independent of myosin II and its associated mechanical activity. In neuroblasts

expressing hypomorphic allele of myosin II's regulatory light chain, sqh^{1}, and in neuroblasts treated with Y-27632, a Rho kinase inhibitor that inactivates myosin II, Par-3/Baz localization is unaffected (Barros *et al.*, 2003). Moreover, actomyosin in neuroblasts appears to be less dynamic than in *C. elegans* embryos. With the exception of being apically enriched during metaphase, other more elaborate actomyosin-driven dynamics such as cortical flow was not observed in cross-sectional live imaging analyses performed in neuroblasts. Given the distinction between the two known Par polarity states–cytoplasmic, unpolarized vs. apical, polarized–in neuroblasts, Par polarization was speculated to occur via a direct, single-step asymmetric-targeting mechanism, that does not involve actomyosin and its associated contractility.

CHAPTER II

ASYMMETRIC RECRUITMENT AND ACTIN DEPENDENT CORTICAL FLOWS DRIVE THE NEUROBLAST POLARITY CYCLE

^ This chapter contains published co-authored material.

C.H. Oon and K.E. Prehoda*

Institute of Molecular Biology, Department of Chemistry and Biochemistry

1229 University of Oregon, Eugene OR 97403

* Corresponding author: prehoda@uoregon.edu

Author Contributions: C.H. Oon contributed to Conceptualization, Data curation, Formal analysis, Investigation, Visualization, Methodology, Writing—review and editing. K.E. Prehoda contributed to Conceptualization, Software, Formal analysis, Supervision, Funding acquisition, Visualization, Methodology, Writing—original draft, Project administration, Writing—review and editing.

INTRODUCTION

Drosophila neuroblasts dynamically polarize to segregate fate determinants while dividing asymmetrically (Homem and Knoblich, 2012; Knoblich, 2010; Prehoda, 2009; Venkei and Yamashita, 2018). Cortical polarization during mitosis allows fate

determinant containing cortical domains to be separated by the cleavage furrow during cytokinesis. Following division, fate determinant segregation causes one daughter cell to retain the neuroblast fate and to undergo further asymmetric divisions, while the other takes on a differentiated fate to populate the central nervous system. The catalytic activity of atypical Protein Kinase C (aPKC), a component of the animal cell polarity Par complex, is central to this process, and must be localized to the neuroblast's apical cortex during mitosis. Phosphorylation of neuronal fate determinants displaces them from the membrane, ensuring that they are restricted to the basal cortex to be segregated into the differentiating daughter cell (Atwood and Prehoda, 2009; Bailey and Prehoda, 2015; Betschinger et al., 2003; Lang and Munro, 2017; Rolls et al., 2003). During each asymmetric neuroblast division, aPKC cycles between polarized and unpolarized states. Here we examine the dynamic processes that underlie aPKC polarization and depolarization during neuroblast asymmetric division cycles.

Neuroblasts begin asymmetric division with aPKC in the cytoplasm (Hannaford et al., 2018). By metaphase, aPKC accumulates at a cortical domain around the apical pole where it directs the polarization of differentiation factors such as Miranda and Numb to the basal cortex (Homem and Knoblich, 2012; Knoblich, 2010; Prehoda, 2009). Preferential targeting of aPKC to the apical cortex could explain neuroblast polarization, although little is known about how this process might occur. Furthermore, asymmetric targeting as a polarization mechanism contrasts with the dynamics of aPKC polarization in the early worm embryo in which aPKC is localized to both the anterior and posterior domains of the worm cortex before sperm entry (Lang and Munro, 2017; Tabuse et al., 1998; Wang et al., 2017). Directional transport from the posterior to anterior cortical

domain (i.e. cortical flow), potentially through the activity of actomyosin (Munro et al., 2004), is thought to play a key role in the worm embryo. It has been unknown whether cortical flows play any role in aPKC polarization in neuroblasts. Furthermore, the nature of the aPKC cortical recruitment process has not been described.

Because neuroblasts repeatedly cycle between polarized (apical aPKC at metaphase) and unpolarized (interphase cytoplasmic aPKC) states, depolarization is a necessary step in the neuroblast polarity cycle (Figure 1A). However, little is known about the events that follow metaphase that regenerate the unpolarized state. These events may be especially important for asymmetric division because the localization of aPKC at metaphase is distant from the site of cleavage furrow formation in anaphase, the exclusion point for basal fate determinants. Understanding how metaphase polarity is disassembled may provide insight into the mechanism by which determinants are prevented from occupying the apical cortex that becomes the self-renewed neuroblast following division.

We have investigated how neuroblasts transition between polarity states – the neuroblast polarity cycle – to gain insight into the mechanisms by which metaphase polarity is formed and disassembled. We have sought to determine whether neuroblast polarity results from direct recruitment from the cytoplasm, or if the process requires additional steps. Likewise, does depolarization occur simply from direct exchange from the apical cortex into the cytoplasm? Furthermore, we have examined the role of the actin cytoskeleton in neuroblast polarization and depolarization. The dynamic steps in neuroblast polarization that we have discovered provide further insight into the

mechanisms underlying animal cell polarity and a new framework for using the neuroblast as a polarity model system.

RESULTS

The neuroblast polarity cycle is a dynamic, multistep process

We investigated the divisions of neuroblasts from *Drosophila* larval brain lobes (Homem and Knoblich, 2012), first focusing on a GFP fusion of aPKC (aPKC-GFP) (Besson et al., 2015), as its catalytic activity is the direct output of the Par complex (Atwood and Prehoda, 2009; Bailey and Prehoda, 2015). We simultaneously imaged an RFP fusion of Histone H2A (RFP-H2A) to assess the cell cycle stage. To identify as much of the dynamics of the neuroblast polarization process as possible, we imaged the process every 20 seconds or faster, the maximum acquisition frequency that yielded sufficient signal and little photobleaching. Furthermore, we collected optical sections throughout the full volume of the cell to visualize sections in the center along with those at the cortical edge and to allow for full three-dimensional projections at each time point. These data reveal a highly dynamic process that begins with aPKC in the cytoplasm as cells entered mitosis (Figure 1B and C; Figure 1–video 1). Near the time when chromosome condensation became apparent, discrete aPKC foci appeared on the cortex, preferentially in apical hemisphere. We also observed aPKC foci in three dimensional projections of fixed, wild type prophase neuroblasts using an anti-aPKC antibody (Figure 1-supplement 1). Near metaphase, the aPKC cortical foci, which by then had grown into larger patches, moved towards the apical pole in a concerted fashion, coalescing into an "apical cap", the metaphase neuroblast polarity state. The aPKC apical cap remained until

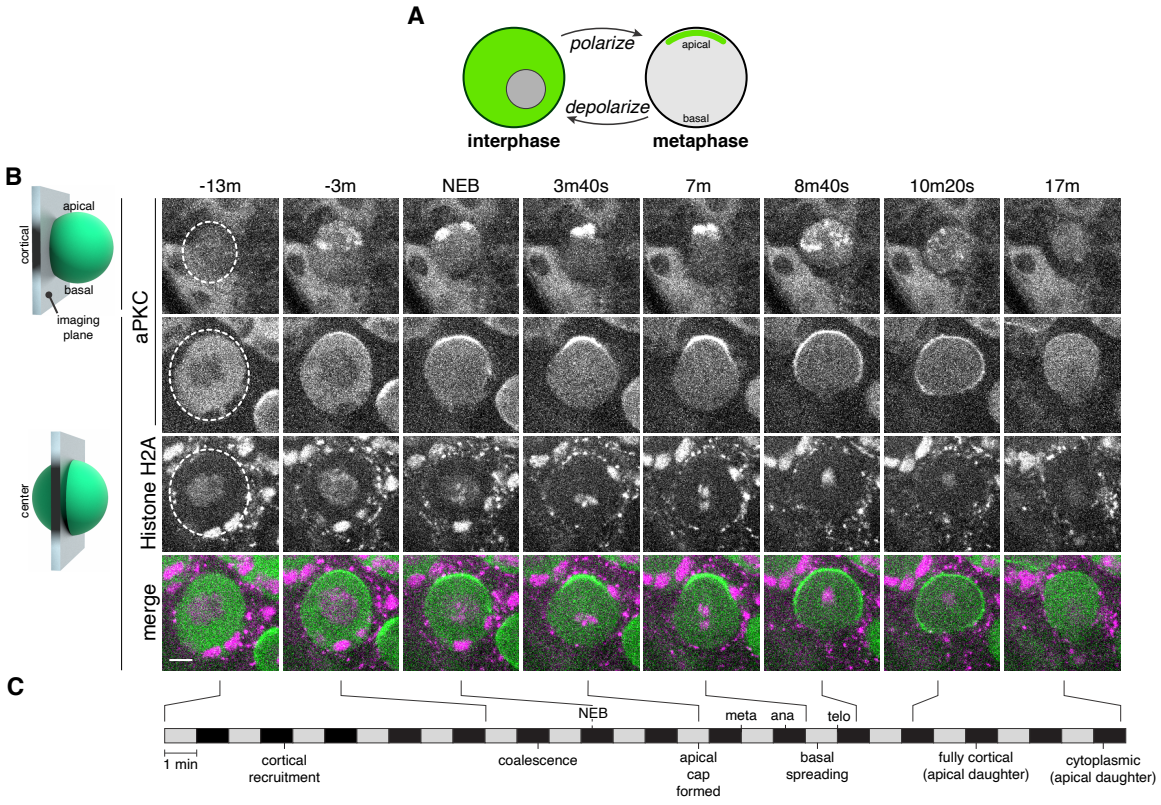

Figure 1 The neuroblast polarity cycle is a dynamic, multistep process. (A) Schematic of the neuroblast polarity cycle. Neuroblasts transition between unpolarized, cytoplasmic aPKC in interphase, to an apical cortical domain tightly focused around the apical pole in metaphase, the canonical neuroblast polarity state, during repeated asymmetric divisions. **(B)** Frames from Figure 1-video 1 showing 1.5 µm maximum intensity projections of aPKC-GFP signal along the cortical edge ("cortical"; top row) and center ("center"; rows 2-4) of a neuroblast. A maximum intensity project of RFP-Histone H2A signal through the center of the cell, along with a merge of GFP and RFP central projections, are also shown. The outline of the neuroblast is highlighted with a dashed line in the first column. Time is shown relative to nuclear envelope breakdown. **(C)** Timeline of the neuroblast polarity cycle with cell cycle hallmarks (NEB, nuclear envelope breakdown; meta, metaphase; ana, anaphase; telo, telophase) marked above the timeline and polarization events below.

shortly after anaphase onset at which point the cap disassembled by rapid spreading of cortical patches towards the contracting cleavage furrow. No aPKC signal was detected on the cortex of the basal ganglion mother cell (Figure 1B; Figure 1–videos 1). In addition, the cortical aPKC in the newborn neuroblast daughter rapidly dissipated into the

cytoplasm at the end of mitosis. The overall polarity cycle, from the initial appearance of cortical foci to dissipation occurred in 28.8 ± 8.2 minutes (n = 20 neuroblasts from four larvae).

These data reveal previously unrecognized complexity in neuroblast polarization and depolarization processes. We speculate that previous studies failed to observe these dynamics because of their transient nature, and furthermore, the discontinuous nature of the cortical aPKC signal is less visible in central optical sections compared to those along the cortical edge (Figure 1B; Figure 1-video 1). In the following sections we examine the neuroblast polarity cycle in more detail.

Asymmetric cortical recruitment yields a discontinuous, unorganized structure

High frame rate projections of the full neuroblast volume revealed that the initial step in aPKC polarization is the formation of discontinuous patches on the apical cortex (Figure 1B; Figure 1–video 1; Figure 2A). Apical targeting begins in early prophase and ends shortly before nuclear envelope breakdown (NEB; as assessed by the appearance of aPKC-GFP in the nucleus) with an overall time of 11.1 ± 6.2 minutes (n = 20). We observed the first small cortical foci in early prophase when chromosome condensation became apparent. Focus formation was heavily biased towards the apical cortical hemisphere (defined by the hemisphere opposite where the smaller ganglion mother cell eventually formed; Figure 2B). Over time the foci grew into patches, both by fusing with other foci and by the recruitment of additional aPKC from the cytoplasm (Figure 2A). Patches generally remained near the location where they initially appeared, undergoing unbiased diffusive movements (Figure 2A,C,D). Although cortical targeting by focus formation occurred predominantly in the apical hemisphere, occasionally we observed

foci in the basal hemisphere. However, these foci either dissipated back into the cytoplasm or became part of the apical cap (see below; Figure 2E).

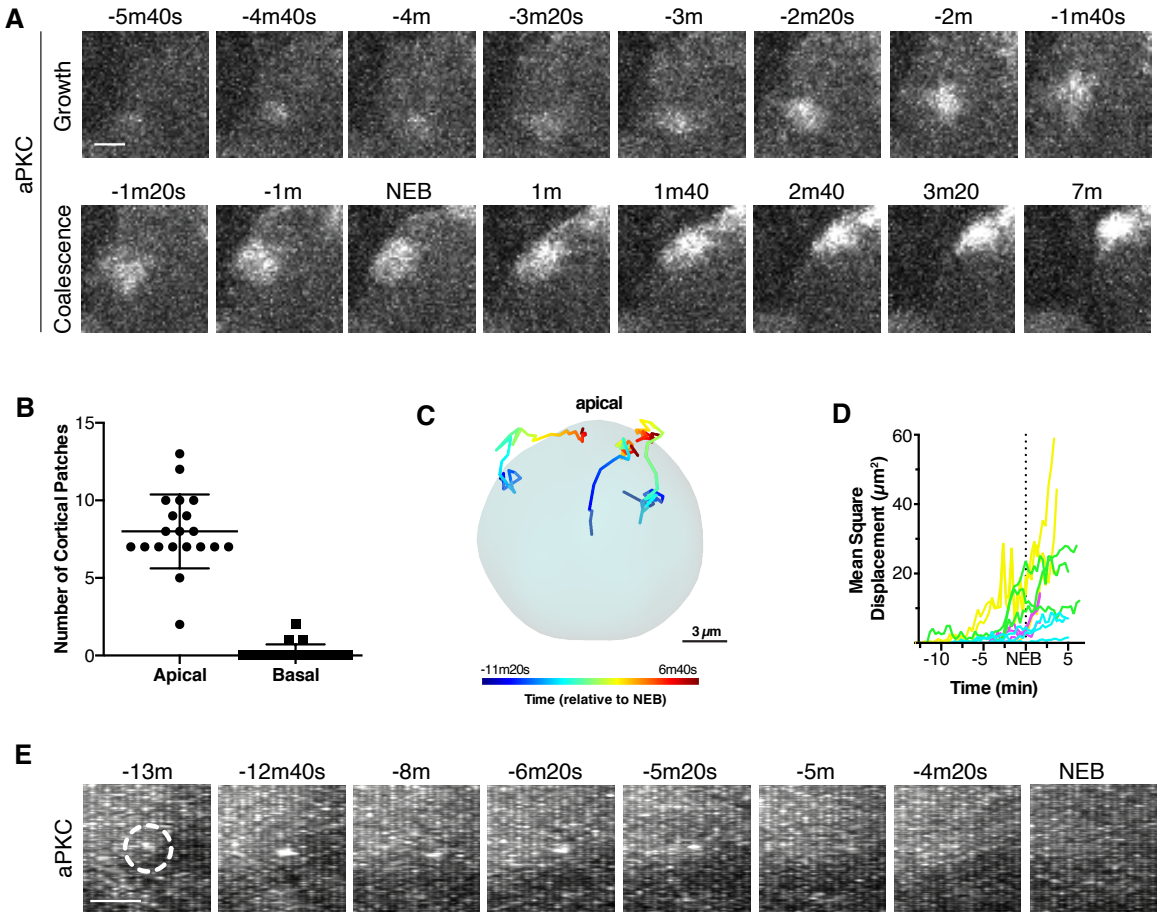

Figure 2 Apically directed cortical recruitment and patch coalescence (A) Example of aPKC-GFP cortical patches during growth and coalescence phases. Scale bar 2 µm. **(B)** The number of aPKC-GFP cortical patches in the apical and basal hemispheres immediately before cortical flow begins. Each point represents a distinct neuroblast (taken from four larvae). Bars represent one standard deviation from the mean. Data are included in Figure 2-source data 1. **(C)** Example patch trajectories during coalescence from particle tracking. Cell outline is shown in light blue. **(D)** Mean square displacement of several different patches identified by particle tracking as a function of time. **(E)** Frames (3 µm maximum intensity projection) from a time series showing the example fate of an aPKC-GFP cortical focus (dashed circle) that appeared in the basal cortical hemisphere and dissipated before NEB. Scale bar 2 µm.

Coordinated flow of cortical aPKC patches leads to formation of a metaphase apical cap

The asymmetric cortical recruitment that occurred in prophase yielded a discontinuous, unorganized apical structure that occupied a large portion of the apical cortical hemisphere. Approximately 90 seconds before NEB, the aPKC patches on the apical cortex, which had been undergoing uncoordinated, seemingly random movements along the cortex, began to move in a highly coordinated fashion towards the apical pole (Figures 1B and 2A, C; Figure 1–video 1). The coordinated movements transformed the broad, discontinuous network of patches into a continuous cap tightly focused around the apical pole. The cap formation process lasted approximately four minutes (3.9 ± 1.1 minutes; n = 20), measured from the point at which coordinated movement begins to when the continuous apical cap is formed (Figures 1B and 2C,D) with patches traveling a mean distance of 4.1 ± 1.8 μm at a mean velocity of 0.02 ± 0.01 μm/s (n = 12). The coordinated nature of aPKC patch movements leads us to term it "cortical flow" because the movement is directed, it occurs at the cell periphery, and resembles the movements that take place in the early worm embryo following fertilization when symmetrically cortical aPKC moves towards the anterior cortex (Munro et al., 2004; Wang et al., 2017). Moreover, as described below, these movements require the actin cytoskeleton. Once the cap is formed it is very stable; we observed little change in aPKC localization over an approximately four-minute period that extended from shortly after nuclear envelope breakdown through metaphase (3.9 ± 0.9 minutes; n = 20).

Apical cap disassembly during anaphase causes aPKC spreading to the cleavage furrow

Shortly after the onset of anaphase, the apical cap underwent a dramatic disassembly event that coincided with the changes in cellular morphology that occur at the end of mitosis (Figure 1B,C; Figure 1–video 1) (Connell et al., 2011; Hickson et al., 2006). The apical cap, which up until this point had remained uniform, began to break apart into individual patches, similar in appearance to those observed before cap formation (Figure 1B and Figure 3; Figure 1–video 1). Cap disassembly coincided with the extension of the apical cortex that occurs during late anaphase and was characterized by spreading of the patches along the cortex towards the site of cleavage furrow formation, with the overall process lasting 3.9 ± 1.0 minutes (n = 20) with patches traveling a mean distance of 6.5 ± 3.3 μm at a mean velocity of 0.04 ± 0.03 μm/s (n = 12). The spreading process appeared similar to the cortical flows that occur during cap formation, although in the basal rather than apical direction. Moreover, the cortex of the budding basal daughter cell did not contain any detectable cortical aPKC signal (Figure 3A). At the end of telophase, the patches that remained on the cortex of the apical daughter cell (which retains the neuroblast fate) rapidly decreased in intensity until no detectable cortical signal remained, regenerating the cytoplasmic aPKC state present at the start of the neuroblast polarity cycle (Figure 3B; Figure 1–video 1).

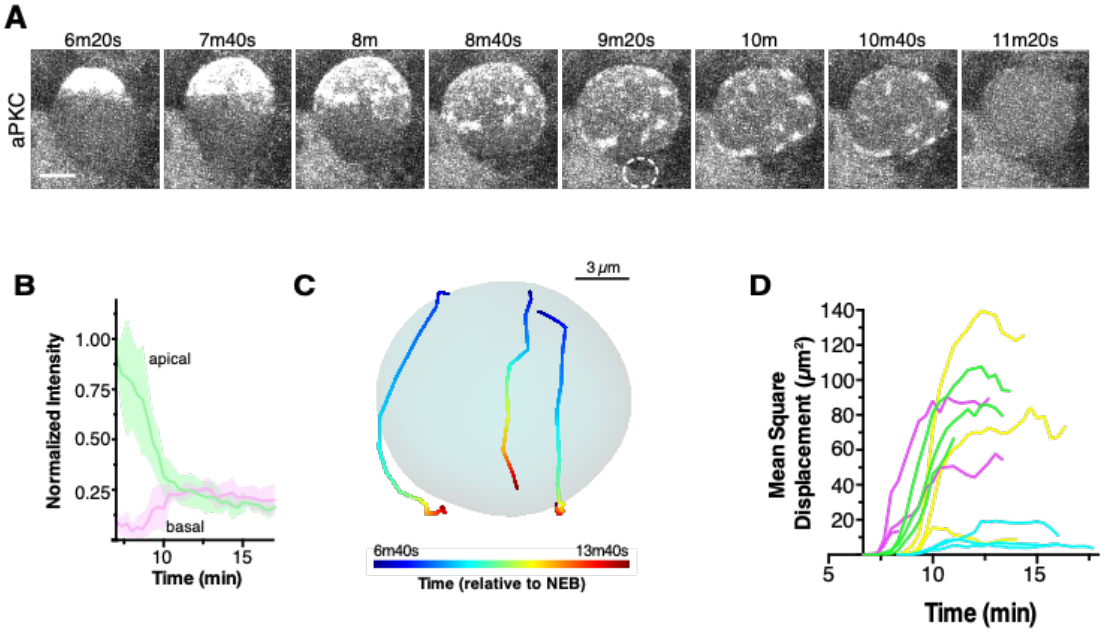

Figure 3 Apical cap disassembly (A) Spreading of aPKC-GFP during cap disassembly and patch dissipation. A 6 µm maximum intensity projection (one hemisphere along the apical-basal axis) is shown in each panel. The time is relative to nuclear envelope breakdown. The position of the budding GMC is shown by a dotted circle as identified from the Histone H2A channel (not shown). Scale bar 5 µm. **(B)** Cortical and cytoplasmic intensity of aPKC-GFP in the apical and basal hemispheres during cap disassembly measured from four neuroblasts (error bars represent one standard deviation). Time is shown relative to NEB. **(C)** Example patch trajectories during cap disassembly from particle tracking. Cell outline is shown in light blue. **(D)** Particle tracking of independent patches reveals their mean square displacement as a function of time (relative to nuclear envelope breakdown).

Apical retention and cortical flows are mediated by the actin cytoskeleton

The dynamic movements of aPKC during the neuroblast polarization and depolarization led us to suspect that the cortical actin cytoskeleton could play important roles in both processes. To investigate whether F-actin participates in the neuroblast polarity cycle, we exposed neuroblasts in various stages of the polarity cycle to the actin depolymerizing drug Latrunculin A (LatA) and imaged the resulting effects on aPKC dynamics.

In neuroblasts treated with LatA during interphase, aPKC appeared in the apical region in early prophase, but in a manner fundamentally different from untreated neuroblasts. In untreated neuroblasts, apical aPKC recruitment occurred primarily via foci appearance and patch growth (Figure 1; Figure 1-video 1) but foci appearance and patch growth in treated neuroblasts was significantly less frequent (Figure 4A and supplement 1; Figure 4–video 1). Furthermore, the foci that did appear often failed to grow into larger patches compared to foci from untreated neuroblasts (Figure 4-supplement 1). Following NEB, cortical aPKC rapidly spread into the basal region before metaphase, a phenomenon that has been previously observed (Hannaford et al., 2018), and failed to undergo coalescence.

LatA treatment of prophase neuroblasts allowed us to examine the effect of loss of the actin cytoskeleton when apical aPKC patches are present on the apical cortex. Once treated with LatA, apical patches failed to undergo further growth and prophase treated neuroblasts nearly always failed to undergo coalescence into an apical cap (Figure 4B and supplement 1; Figure 4–video 2). Similar to interphase treated neuroblasts, aPKC polarity was lost by cortical spreading into the basal domain before metaphase. Interestingly cortical patches present at the apical cortex before treatment ceased movement following LatA addition (Figure 4B,C; Figure 4-videos 1 and 2) and did not spread into the basal domain, indicating that aPKC depolarization results from spreading of non-patch associated protein.

Neuroblasts treated with LatA near the time at which aPKC patches coalesce into an apical cap exhibited limited cap dissociation unlike in untreated neuroblasts where the aPKC cap dissociated into patches that rapidly spread to the cleavage furrow (Figure 4C

and supplement 1; Figure 4–video 3). In metaphase treated neuroblasts, we observed some breakup of the cap, but most patches remained near the apical pole before dissipating. LatA treated cells also failed to undergo the morphological changes that normally occur during anaphase in which the apical membrane rapidly extends (Connell et al., 2011) (Figure 4C; Figure 4–video 3).

Together, these data indicate that the actin cytoskeleton participates in multiple phases of the neuroblast polarity cycle. First, while the actin cytoskeleton is not required for asymmetric recruitment to the apical cortex, it does play a key role in the discontinuous structure of foci and apical patches that normally form in prophase. Furthermore, the actin cytoskeleton is also required to retain aPKC at the apical cortex as LatA treatment causes aPKC to rapidly spread onto the basal cortex before metaphase, although aPKC that had been incorporated into patches did not appear to migrate into the basal domain (Figure 4B; Figure 4–video 2). Finally, the rapid dynamics of the apical cap – both its formation via coalescence and its disassembly during anaphase – depend nearly completely on the presence of the actin cytoskeleton.

Figure 4 (next page) aPKC cortical dynamics following disruption of the actin cytoskeleton (A) Effect of treating a neuroblast with LatA beginning in interphase (24m20s prior to NEB) on aPKC localization dynamics. Frames from Figure 4–video 1 are shown as 4 μm maximum intensity projections along the cortical edge and center of aPKC-GFP taken from Figure 4-video 1. The cortical projections from an untreated neuroblast at equivalent time points are shown for reference in the top row. The neuroblast is highlighted by a dashed circle in the first column. Time is shown relative to nuclear envelope breakdown (NEB). Scale bar 5 μm. **(B)** Effect of treating a neuroblast with LatA following the initial cortical recruitment events (7m20s prior to NEB) on aPKC localization dynamics. Frames from Figure 4–video 2 are shown as in panel A. **(C)** Effect of treating a neuroblast with LatA following cap coalescence (4m prior to NEB) on aPKC localization dynamics. Frames from Figure 4–video 3 are shown as in panel A.

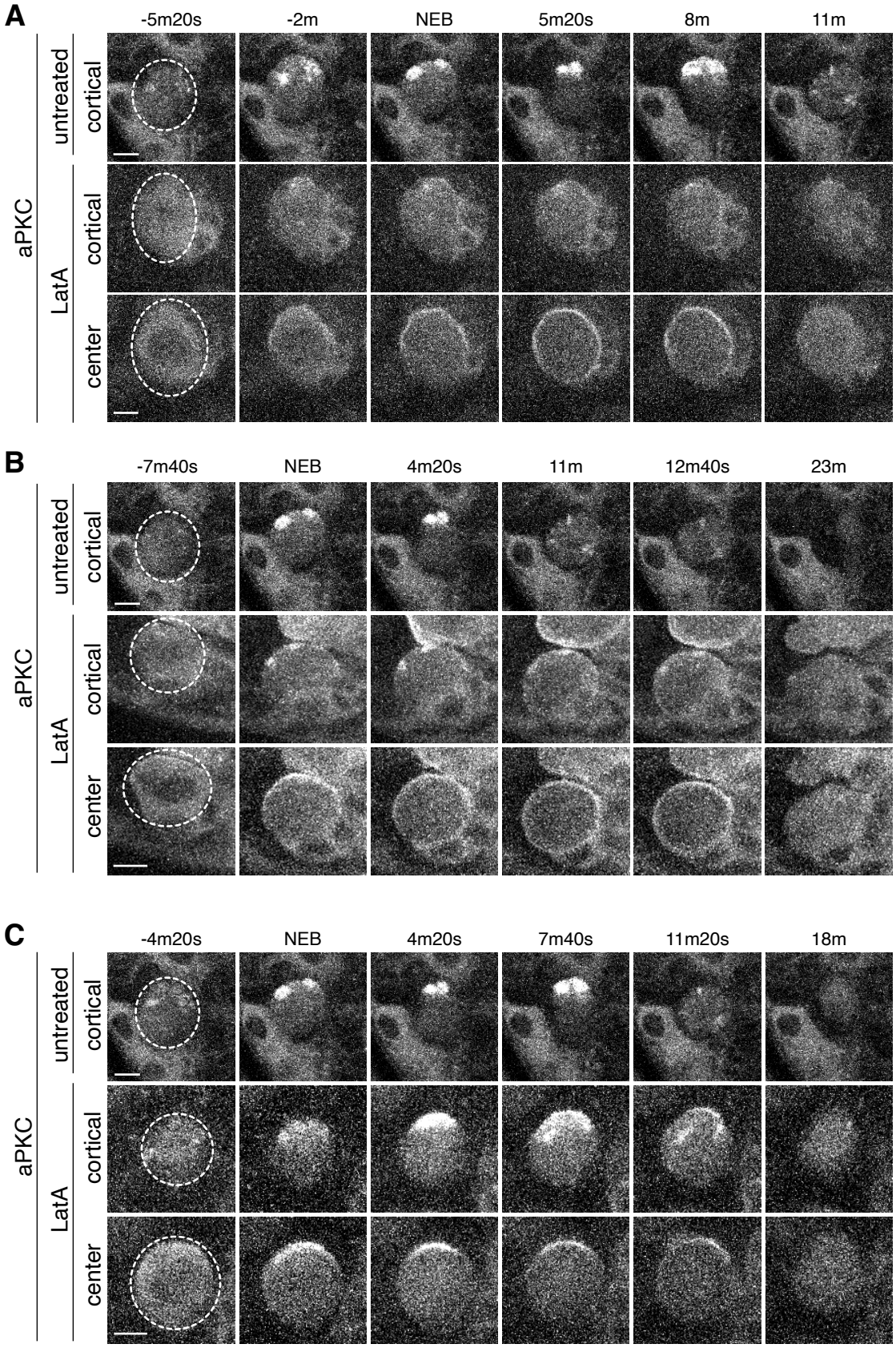
A
-5m20s
-2m
NEB
5m20s
8m
11m
aPKC
untreated
cortical
LatA
cortical
center
B
-7m40s
NEB
4m20s
11m
12m40s
23m
aPKC
untreated
cortical
LatA
cortical
center
C
-4m20s
NEB
4m20s
7m40s
11m20s
18m
aPKC
untreated
cortical
LatA
cortical
center

Actin dependent cortical dynamics of the Par complex regulator Bazooka

The polarization of aPKC requires the activity of Bazooka (Baz; aka Par-3) (Joberty et al., 2000; Rolls et al., 2003; Tabuse et al., 1998; Wodarz et al., 2000). We analyzed the dynamics of a Baz GFP fusion from a gene trap line (Buszczak et al., 2007) to determine if its polarization utilizes similar steps to those we identified for aPKC. We were not able to obtain adequate brightness and photostability with "red" fluorescent protein variants at the frame rates required to observe aPKC dynamics (except for highly abundant proteins like Histone H2A), precluding simultaneous imaging of both proteins. Imaging of neuroblast asymmetric divisions monitoring Baz-GFP revealed that Baz undergoes dynamics that resemble those of aPKC, but with some noticeable differences (Figure 5A,B; Figure 5–video 1). Like aPKC, Baz appears to form a discontinuous apical cortical structure during prophase that coalesces to form an apical cap at metaphase with subsequent disassembly. Based on maximum intensity projections of fixed preparations stained with anti-Baz and anti-aPKC antibodies, patches of the two proteins colocalize at early phases of mitosis, although some Baz patches do not have a corresponding aPKC signal (Figure 5C).

While Baz's dynamics closely resembled aPKC's, we noticed one significant difference. At mitotic entry aPKC's localization is exclusively cytoplasmic, and while Baz is also found in the cytoplasm during this phase of the cell cycle, we also observed a significant number of cortical puncta (Figure 5A; Figure 5–video 1). Baz puncta were relatively stationary and many, especially those at the apical cortex, disappeared near mitotic entry. Those with longer lifetimes that persisted into mitosis did not participate in cap coalescence. Shortly after cytokinesis, new puncta often appeared.

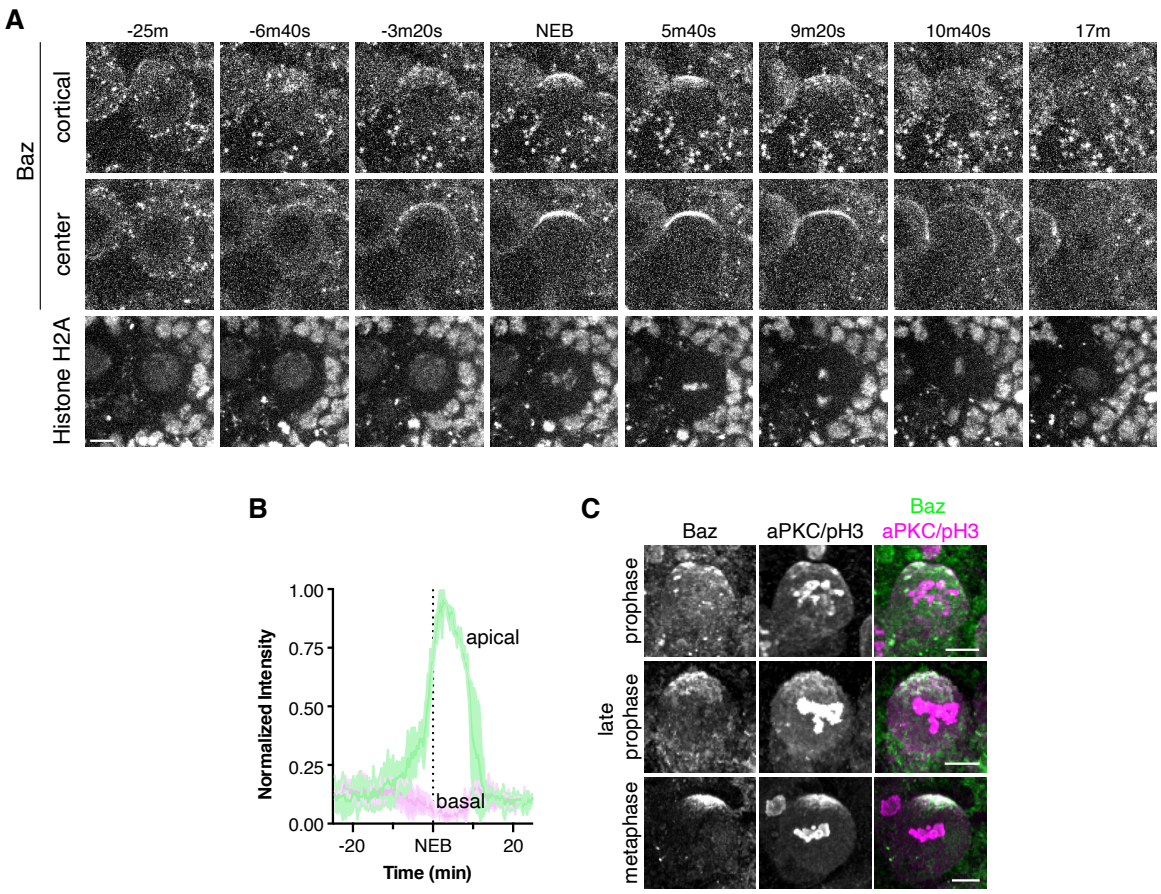

Figure 5 Bazooka dynamics during the neuroblast polarity cycle (A) Frames from Figure 5–video 1 showing 4 µm maximum intensity projections through the cortical edge and center of a larval brain neuroblast expressing Baz-GFP. A central projection of Histone H2A fusion to RFP is shown in the bottom row. The time relative to nuclear envelope breakdown ("NEB") is shown. Scale bar 5 µm. **(B)** Normalized apical and basal cortical intensity (see methods) of Baz-GFP as a function of time relative to NEB from the divisions of three different neuroblasts with the mean and standard deviation of the signal shown. **(C)** Localization of Baz and aPKC in fixed neuroblasts at early stages of mitosis (pH3 = phospho-histone H3).

We also examined the effect of LatA induced depolymerization of the actin cytoskeleton on Baz's dynamics. In cells treated before metaphase, the appearance of Baz apical patches was reduced following treatment and those that did appear failed to coalesce in most cases, similar to LatA's effect on aPKC dynamics (Figure 6A,B and supplement 1; Figure 6-videos 1,2). However, while LatA treatment induced spreading of

apically enriched aPKC onto the basal cortex, apically recruited Baz remained predominantly in the apical hemisphere following treatment. For neuroblasts treated with LatA near the time of apical cap formation, we observed little Baz cap disassembly, similar to the effect on aPKC's cap (Figure 6C and supplement 1; Figure 6-videos 3). Our results indicate that the actin cytoskeleton plays a similar role in Baz and aPKC polarization dynamics suggesting that they are polarized by similar mechanisms. However, the actin cytoskeleton appears to be less important for the maintenance of Baz's polarity early in mitosis than it is for aPKC's as LatA did not induce Baz spreading onto the basal cortex.

Figure 6 (next page) Baz cortical dynamics following disruption of the actin cytoskeleton (A) Effect of treating a neuroblast with LatA beginning in interphase (83m20s before NEB) on Baz localization dynamics. Frames from Figure 6–video 1 are shown as 4 μm maximum intensity projections along the cortical edge and center of Baz-GFP taken from Figure 4-video 1. The cortical projections from an untreated neuroblast at equivalent time points are shown for reference in the top row. The neuroblast is highlighted by a dashed circle in the first column. Time is shown relative to nuclear envelope breakdown (NEB). Scale bar 5 μm. **(B)** Effect of treating a neuroblast with LatA following the initial cortical recruitment events (7m40s prior to NEB) on Baz localization dynamics. Frames from Figure 6–video 2 are shown as in panel A. **(C)** Effect of treating a neuroblast with LatA following cap coalescence (30s prior to NEB) on Baz localization dynamics. Frames from Figure 6–video 3 are shown as in panel A.

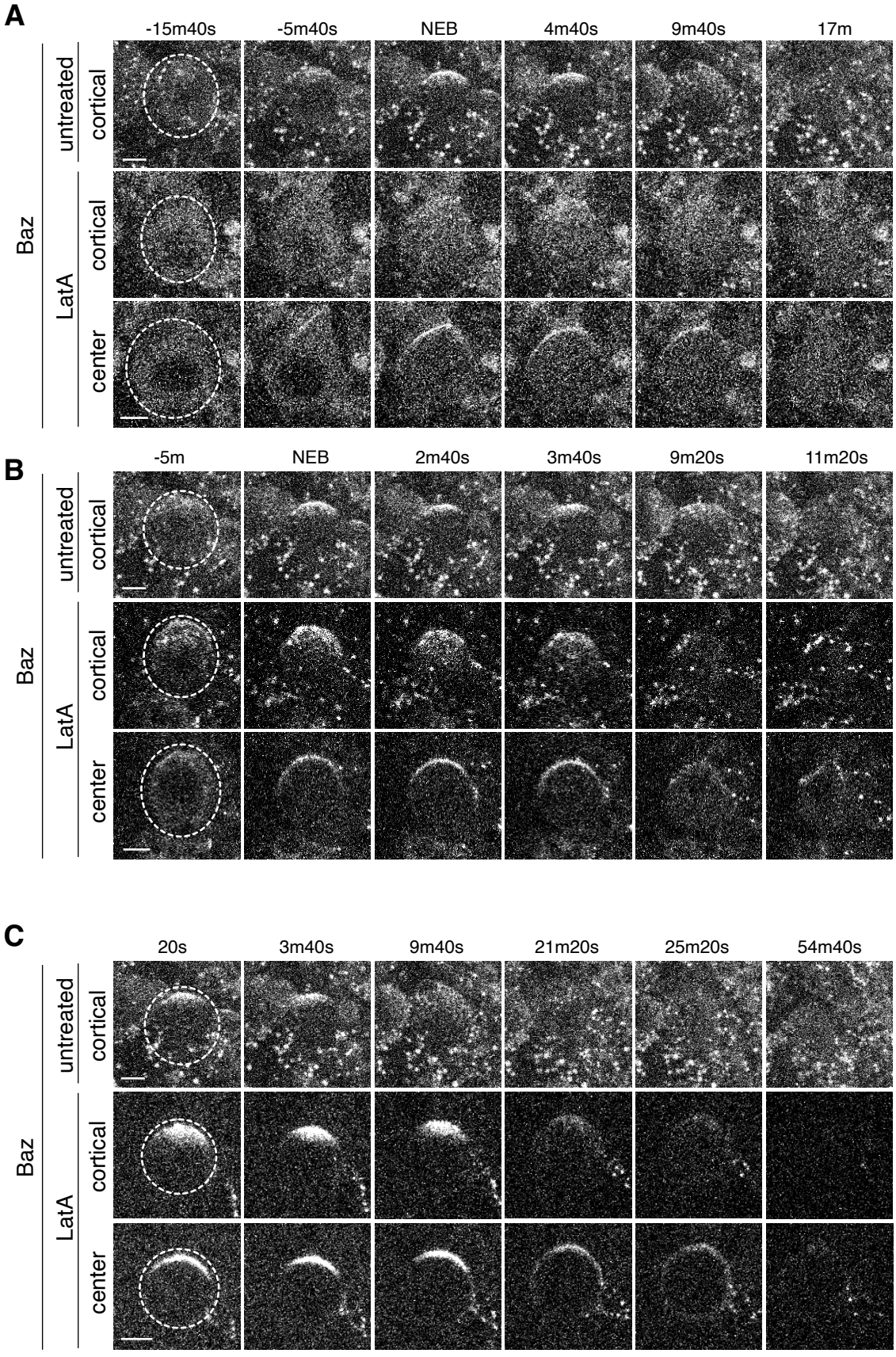
A
-15m40s
-5m40s
NEB
4m40s
9m40s
17m
Baz
untreated
cortical
LatA
cortical
center
B
-5m
NEB
2m40s
3m40s
9m20s
11m20s
Baz
untreated
cortical
LatA
cortical
center
C
20s
3m40s
9m40s
21m20s
25m20s
54m40s
Baz
untreated
cortical
LatA
cortical
center

DISCUSSION

We examined the dynamics that accompany transitions between unpolarized and polarized states of *Drosophila* neuroblasts using rapid imaging throughout the full volume of the cell. These data reveal that canonical neuroblast polarity, with the Par complex's catalytic component aPKC tightly localized around the apical pole at metaphase, results from a multistep process (Figure 7). Initially, asymmetric recruitment to the apical cortex leads to a discontinuous structure composed of apical cortical patches. Coordinated cortical flows that begin late in prophase leads to coalescence of the patches into an apical cap. We also discovered a remarkably dynamic depolarization step following metaphase polarity in which the apical cap is broken up into cortical patches that spread to the cleavage furrow and ultimately dissipate back into the cytoplasm (Figure 7). We examined the role of the actin cytoskeleton in the steps that make up the neuroblast polarity cycle and found that it is critical for several different aspects of polarization and depolarization.

In principle, cortical polarity could result from directional cortical flow of initially symmetric cortical molecules, or from asymmetric cortical targeting directly from the cytoplasm. In the early worm embryo, aPKC is initially symmetrically localized to evenly distributed cortical foci (Munro et al., 2004; Wang et al., 2017). The cortical cue provided by sperm entry induces anterior directed flows that deplete aPKC foci from the posterior cortex and concentrate it in the anterior hemisphere (Rose and Gönczy, 2014). In contrast to the early worm embryo, neuroblasts begin their polarization cycle with cytoplasmic aPKC (Figure 7) such that asymmetry in the cortical recruitment process could be sufficient for polarization. We observed that neuroblast polarity begins with

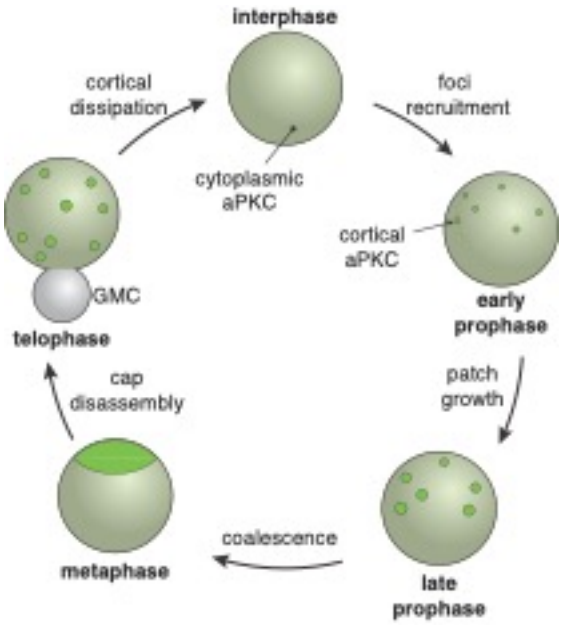

Figure 7 The neuroblast polarity cycle. The cycle begins with discontinuous patches of aPKC forming in the apical hemisphere via recruitment to the cortex from the cytoplasm. The aPKC cap observed in metaphase neuroblasts is formed from coordinated cortical flows that lead to coalescence of the discontinuous patches into a uniform structure tightly localized around the apical pole. During anaphase, the cap is disassembled leading to discontinuous spreading that extends to the cleavage furrow, followed by cortical dissipation back into the cytoplasm.

asymmetric recruitment but that this process alone leads to a discontinuous polarized structure in the apical hemisphere. Coordinated cortical flows towards the apical pole that begin near metaphase and resemble the polarization of the early worm embryo, transform this unorganized structure into the tightly focused metaphase polarity state. Thus, neuroblast polarity results not from a single process, but from the stepwise activity of two very different cellular processes: asymmetric targeting and actin dependent cortical flow.

Given that neuroblasts undergo repeated asymmetric divisions, the neuroblast polarity cycle also includes a depolarization step to regenerate cytoplasmic aPKC, the initial state in the cycle. Rather than directly returning to the cytoplasm from the apical cap, we observed a dramatic cap disassembly step that appears similar to the assembly

step but in reverse: the cap breaks up into aPKC patches that move towards the basal rather than apical pole. We speculate that cap disassembly may play an especially important role in segregating fate determinants by extending aPKC fully along the cortex to the cleavage furrow, but not beyond. Cortical spreading of aPKC could provide a mechanism for ensuring basal fate determinants such as Miranda and Numb are completely excluded from the cortex that becomes part of the self-renewed neuroblast following cytokinesis. Is cap disassembly an active process? As it is initiated precisely when the dramatic morphologic changes in anaphase occur (Connell et al., 2011), it may be that this step utilizes a passive mechanism, in which disassembly is driven by the mechanical stresses that the cortex undergoes during this step of the cell cycle.

The cycle we have identified here represents a new framework for understanding the mechanisms that regulate neuroblast polarity. We have begun to utilize this framework to examine the role the actin cytoskeleton plays in the polarity cycle. While the actin cytoskeleton has been known to be required for metaphase polarity for some time with normally apical proteins such as Inscuteable becoming fully cortical at metaphase when actin filaments are depolymerized (Broadus and Doe, 1997), its precise role has been unclear. Here we find that the fully cortical depolarized state can result from a polarized intermediate: in interphase treated neuroblasts aPKC is asymmetrically recruited during prophase but rapidly spreads onto the basal cortex. Thus, at least for aPKC, the actin cytoskeleton is not required for polarized cortical recruitment, but is instead necessary for retention at the apical cortex. Treatment of neuroblasts with LatA at various stages of the cell cycle also revealed that the coalescence of aPKC and Baz patches into a metaphase apical cap and cap disassembly both require an intact actin

cytoskeleton. We suspect that the analysis of other perturbations in terms of the neuroblast polarity cycle, such as mutants of previously described polarity genes, will lead to new insight into the mechanisms by which animal cells become polarized.

MATERIALS AND METHODS

Fly strains and genetics

Oregon R flies were used for examining the localization of fixed endogenous proteins. For live imagine, BAC-encoded aPKC-GFP flies (Besson et al., 2015) and a Baz GFP gene trap line (Buszczak et al., 2007) were used for assessing aPKC and Baz localization and dynamics, respectively. Each were crossed with a His2A-RFP line (Bloomington stock 23650).

Live imaging

Third instar larvae were dissected to isolate the brain lobes and ventral nerve cord, which were placed in Schneider's Insect media (SIM). Larval brain explants were placed in lysine-coated 35 mm cover slip dishes (WPI) containing modified minimal hemolymph-like solution (HL3.1). Treated and untreated explants were imaged on a Leica DMi8 microscope (100x 1.4 NA oil-immersion objective) equipped with a Yokogawa CSU-W1 spinning disk head and dual Andor iXon Ultra camera. Explants expressing aPKC-GFP or Baz-GFP were illuminated with 488 nm and 561 nm laser light throughout 41 optical sections with step size of 0.5 μm and time interval of 20 seconds. To examine the role of F-actin in aPKC and Baz dynamics, explants were treated with 50 μM LatA (2% DMSO) during imaging.

Immunofluorescent staining

Intact brain lobes and ventral nerve cord dissected in SIM from third instar *Oregon R* larvae were fixed in 4% PFA and stained with rabbit anti-PKC ζ primary (C20; 1:1000; Santa Cruz Biotechnology Inc.) and 647 anti-rabbit secondary antibodies (Jackson ImmunoResearch Laboratories) to determine native aPKC localization. Native Baz localization were assessed in third instar *Oregon R* larval brains that were fixed and stained with guinea pig anti-Baz primary (1:1000; (Siller et al., 2006)) and 488 anti-guinea pig secondary antibodies (Invitrogen). The cell cycle stage was assessed with rabbit anti-phospho Histone H3 primary (1:2000 ;Millipore) and 405 anti rabbit secondary (Jackson ImmunoResearch Laboratories). Confocal images were acquired on an Olympus Fluoview FV1000 microscope equipped with a 40x 1.3 NA oil-immersion objective.

Image processing and visualization

Movies were analyzed in ImageJ (using the FIJI package) and in Imaris (Bitplane). Neuroblasts whose apical-basal polarity axis is positioned parallel to the imaging plane were cropped out to generate representative images and movies. Cortical edge and central maximum intensity projections (MIP) were derived from optical slices capturing the surface and center of the cell, respectively. Optical sections capturing the whole of the cell were assembled for 3D rendering and visualization in Imaris. These volumetric representations were used to quantify the time interval of each process within the polarity cycle and the number of patches recruited to the cortex before cortical flow. Patches that were 0.85 μm^2 or larger were selected for quantification.

Intensity measurements

Intensity profiles were measured in FIJI using a 3 μm line across the apical and basal cortex of 4 μm maximum intensity projections through the center of the neuroblast. Mean signal intensities at time *t* are normalized using the following equation:

$$I_{normalized}(t) = \frac{I_{mean}(t) - I_{min}}{I_{max} - I_{min}}$$

where I_{mean} is the average intensity within the region specified by the line scan at time *t*, I_{min} is the minimum mean intensity measured across the entire dataset, and I_{max} is the maximum mean intensity measured across the entire dataset.

Particle tracking

The timing of dynamic events within the aPKC polarity cycle was determined using the H2A channel. Cortical patches were tracked through cap formation and cap dissociation using the Imaris Spots module. Tracking was restricted by an intensity threshold set by the average intensity of the apical cap in metaphase to help increase accuracy of the tracking algorithm. Smaller, lower intensity foci that grew into patches were tracked manually and their tracks were linked to that of the corresponding patches to construct a fully assembled, continuous track. Statistical data such as total patch displacement, mean square patch displacement, and relative speed between time points were collected from the final tracking result. Mean patch speed for cap assembly were calculated using a 160 second time window starting at the onset of cortical flow. Mean patch speed for cap disassembly were calculated using a 160 second time window start at the onset of disassembly.

VIDEO LEGENDS

Figure 1–video 1. Localization dynamics of the Par complex component aPKC during neuroblast asymmetric division.

Montage of maximum intensity projections of aPKC-GFP signal from a *Drosophila* larval brain neuroblast through the entire cell (upper left), cortical edge (upper right), and center (lower right). Histone H2A-RFP signal is shown in the bottom left. Time is relative to nuclear envelope breakdown.

Figure 4–video 1. Effect of interphase LatA treatment on aPKC localization dynamics.

A neuroblast is shown from a *Drosophila* larval brain explant treated with LatA 24 minutes and 20 seconds before the neuroblast underwent nuclear envelope breakdown. The montage includes maximum intensity projections of aPKC-GFP signal through the entire cell (upper left), cortical edge (upper right), and center (lower right). Histone H2A-RFP signal is shown in the bottom left. Time is relative to nuclear envelope breakdown.

Figure 4–video 2. Effect of LatA treatment following cortical recruitment on aPKC localization dynamics.

A neuroblast is shown from a *Drosophila* larval brain explant treated with LatA 7 minutes and 20 seconds before the neuroblast underwent nuclear envelope breakdown. The montage includes maximum intensity projections of aPKC-GFP signal through the entire cell (upper left), cortical edge (upper right), and center (lower right). Histone H2A-RFP signal is shown in the bottom left. Time is relative to nuclear envelope breakdown.

Figure 4–video 3. Effect of LatA treatment following apical cap coalescence on aPKC localization dynamics.

A neuroblast is shown from a *Drosophila* larval brain explant treated with LatA 4 minutes before the neuroblast underwent nuclear envelope breakdown. The montage includes maximum intensity projections of aPKC-GFP signal through the entire cell (upper left), cortical edge (upper right), and center (lower right). Histone H2A-RFP signal is shown in the bottom left. Time is relative to nuclear envelope breakdown.

Figure 5–video 1. Localization dynamics of the Par complex regulator Baz during neuroblast asymmetric division.

Montage of maximum intensity projections of Baz-GFP signal from a *Drosophila* larval brain neuroblast through the entire cell (upper left), cortical edge (upper right), and center (lower right). Histone H2A-RFP signal is shown in the bottom left. Time is relative to nuclear envelope breakdown.

Figure 6–video 1. Effect of interphase LatA treatment on Baz localization dynamics.

A neuroblast is shown from a *Drosophila* larval brain explant treated with LatA 83 minutes and 20 seconds before the neuroblast underwent nuclear envelope breakdown. The montage includes maximum intensity projections of Baz-GFP signal through the entire cell (upper left), cortical edge (upper right), and center (lower right). Histone H2A-RFP signal is shown in the bottom left. Time is relative to nuclear envelope breakdown.

Figure 6–video 2. Effect of LatA treatment following cortical recruitment on Baz localization dynamics.

A neuroblast is shown from a *Drosophila* larval brain explant treated with LatA 7 minutes and 40 seconds before the neuroblast underwent nuclear envelope breakdown. The montage includes maximum intensity projections of Baz-GFP signal through the

entire cell (upper left), cortical edge (upper right), and center (lower right). Histone H2A-RFP signal is shown in the bottom left. Time is relative to nuclear envelope breakdown.

Figure 6–video 3. Effect of LatA treatment following apical cap coalescence on Baz localization dynamics.

A neuroblast is shown from a *Drosophila* larval brain explant treated with LatA 30 seconds before the movie begins. The montage includes maximum intensity projections of Baz-GFP signal through the entire cell (upper left), cortical edge (upper right), and center (lower right). Histone H2A-RFP signal is shown in the bottom left. Time is relative to nuclear envelope breakdown.

CHAPTER III

PHASES OF CORTICAL ACTOMYOSIN DYNAMICS THAT UNDERLIE THE NEUROBLAST POLARITY CYCLE

^ This chapter contains unpublished co-authored material.

C.H. Oon and K.E. Prehoda*

Institute of Molecular Biology, Department of Chemistry and Biochemistry

1229 University of Oregon, Eugene OR 97403

* Corresponding author: prehoda@uoregon.edu

Author Contributions: C.H. Oon contributed to Conceptualization, Data curation, Formal analysis, Investigation, Visualization, Methodology, Writing—review and editing. K.E. Prehoda contributed to Conceptualization, Data curation, Formal analysis, Investigation, Supervision, Funding acquisition, Visualization, Methodology, Writing—original draft, Project administration, Writing—review and editing.

INTRODUCTION

The Par complex polarizes animal cells by excluding specific cortical factors from the Par cortical domain (Lang and Munro, 2017; Venkei and Yamashita, 2018). In *Drosophila* neuroblasts, for example, the Par domain forms at the apical cortex during

mitosis where it prevents the accumulation of cortical neuronal fate determinants, effectively restricting them to the basal cortex. The resulting cortical domains are bisected by the cleavage furrow segregating neuronal fate determinants into the basal daughter cell where they promote differentiation (Homem and Knoblich, 2012). It was recently discovered that apical Par polarization in the neuroblast is a multistep process in which the complex is initially targeted to the apical hemisphere early in mitosis where it forms a discontinuous meshwork (Kono et al., 2019; Oon and Prehoda, 2019). Cortical Par proteins then move along the cortex towards the apical pole, ultimately leading to formation of an apical cap that is maintained until shortly after anaphase onset (Oon and Prehoda, 2019). Here we examine how the cortical movements that initiate and potentially maintain neuroblast Par polarity are generated.

An intact actin cytoskeleton is known to be required for the movements that polarize Par proteins to the neuroblast apical cortex, but its role in the process has been unclear. Depolymerization of F-actin causes apical aPKC to spread to the basal cortex (Hannaford et al., 2018; Oon and Prehoda, 2019), prevents aPKC coalescence, and induces disassembly of the apical aPKC cap (Oon and Prehoda, 2019), suggesting that actin filaments are important for both apical polarity initiation and its maintenance. How the actin cytoskeleton participates in polarizing the Par complex in neuroblasts has been unclear, but actomyosin plays a central role in generating the anterior Par cortical domain in the *C. elegans* zygote. Contractions oriented towards the anterior pole transport the Par complex from an evenly distributed state (Illukkumbura et al., 2019; Lang and Munro, 2017). Bulk transport is mediated by advective flows generated by highly dynamic, transient actomyosin accumulations on the cell cortex (Goehring et al., 2011a). While

cortical movements of actomyosin drive formation of the Par domain in the worm zygote, and F-actin is required for apical Par polarity in the neuroblast, no apically-directed cortical actomyosin dynamics have been observed during the neuroblast polarization process, despite extensive examination (Barros et al., 2003; Cabernard et al., 2010; Connell et al., 2011; Koe et al., 2018; Roth et al., 2015; Roubinet et al., 2017; Tsankova et al., 2017). Instead, both F-actin and myosin II have been reported to be cytoplasmic or uniformly cortical in interphase, and apically enriched at metaphase (Barros et al., 2003; Koe et al., 2018; Tsankova et al., 2017), before undergoing cortical flows towards the cleavage furrow that are important for cell size asymmetry (Cabernard et al., 2010; Connell et al., 2011; Roubinet et al., 2017).

The current model for neuroblast actomyosin dynamics is primarily based on the analysis of fixed cells or by imaging a small number of central optical sections in live imaging experiments and we have recently found that rapid imaging of the full neuroblast volume can reveal dynamic phases of protein movements (Oon and Prehoda, 2019). Here we use rapid full volume neuroblast imaging to investigate whether cortical actomyosin dynamics occur during early mitosis when the Par complex is polarized.

RESULTS AND DISCUSSION

Pulsatile dynamics of cortical actin during neuroblast asymmetric divisions

To gain insight into how actin participates in the neuroblast polarity cycle, we imaged larval brain neuroblasts expressing an mRuby fusion of the actin sensor LifeAct (mRuby-LA) using spinning disk confocal microscopy. The localization of this sensor in neuroblasts has been reported (Abeysundara et al., 2018; Roubinet et al., 2017), but only

during late mitosis. To follow cortical actin dynamics across full asymmetric division cycles, we collected optical sections through the entire neuroblast volume (~40 0.5 μm sections) at 10 second intervals beginning in interphase and through at least one mitosis (Figure 8-figure supplement 1). Acquiring full cell volume optical sections at this frequency required careful optimization to prevent photobleaching while maintaining sufficient signal levels. Maximum intensity projections constructed from these data revealed localized actin enrichments on the cortex, some of which were highly dynamic (Figure 8 and Figure 8-Video 1). We observed four discrete phases of cortical actin dynamics during neuroblast asymmetric divisions that we describe in detail below.

The interphase neuroblast cortex was a mixture of patches of concentrated actin, highly dynamic pulsatile waves that traveled across the entire width of the cell, and areas with little to no detectable actin (Figure 8 and Figure 8-Video 1). Pulsatile movements consisted of irregular patches of actin forming on the cortex and rapidly moving across the surface before disappearing (Figure 8A,E). Concentrated actin patches were relatively static, but sometimes changed size over the course of several minutes. Static patches were mostly unaffected by the pulsatile waves that occasionally passed over them. Pulses were sporadic in early interphase but became more regular near mitosis, with a new pulse appearing immediately following the completion of the prior one (Figure 8E and Figure 8-Video 1). The direction of the pulses during interphase was highly variable, but often along the cell's equator (i.e. orthogonal to the polarity/division axis). In general, actin in the interphase cortex was highly discontinuous and included large areas with little to no detectable actin in addition to the patches and dynamic pulses described above. Interphase pulses were correlated with cellular scale morphological deformations in

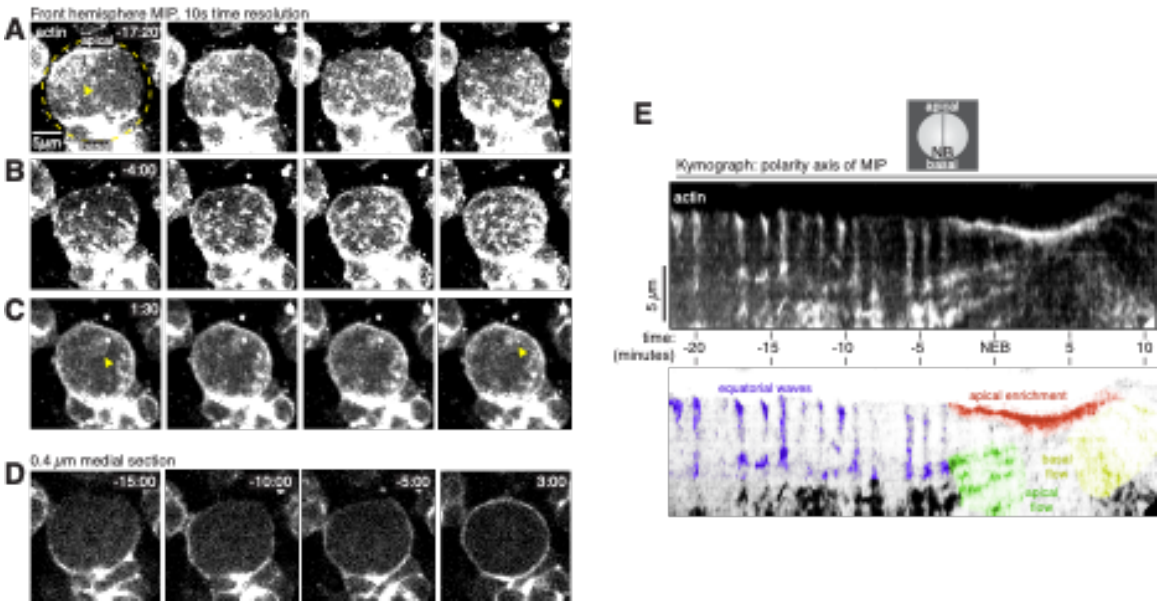

Figure 8 Cortical F-actin dynamics in asymmetrically dividing Drosophila larval brain neuroblasts. (A) Selected frames from Figure 8-Video 1 showing cortical actin pulses during interphase. mRuby-LifeAct expressed via insc-GAL4/UAS ("actin") is shown via a maximum intensity projection (MIP) constructed from optical sections through the front hemisphere of the cell. The outline of the neuroblast is shown by a dashed yellow circle. Arrowhead marks an example cortical actin patch. Time (mm:ss) is relative to nuclear envelope breakdown. **(B)** Selected frames from Figure 8-Video 1 as in panel A showing cortical actin moving apically. **(C)** Selected frames from Figure 8-Video 1 as in panel A showing cortical actin enriched on the apical cortex. **(D)** Selected frames from Figure 8-Video 1 showing how actin becomes cortically enriched near NEB. Medial cross sections show the cortical actin signal is relatively discontinuous until NEB approaches. **(E)** Kymograph constructed from frames of Figure 8-Video 1 using sections along the apical-basal axis as indicated. A legend for the features in the kymograph is included below.

which these areas of low actin signal were displaced away from the cell center while the cortex containing the actin pulse was compressed towards the center of the cell (Figure 8D and Figure 8-Video 1).

Several minutes before nuclear envelope breakdown (NEB) cortical actin dynamics transitioned from unoriented pulses to more sustained movements directed towards the apical pole (-3.4 ± 1.1 minutes; n = 13 from 5 larvae) (Figure 8B-E and Figure 8-Video 1). The interphase pulses we observed were sporadic and relatively

unoriented, but the apically-directed movements that began shortly before NEB (-1.9 ± 1.0 minutes; n = 13 from 5 larvae) were highly regular and apically-directed (i.e. along the polarity/division axis). This phase of cortical actin dynamics continued until anaphase, and was associated with accumulation at the apical cortex as previously described (Barros et al., 2003; Tsankova et al., 2017). Additionally, while the interphase cortex had areas with very little actin, actin was more evenly-distributed following the transition (Figure 8D and Figure 8-Video 1). Another rapid transition occurred shortly after anaphase onset, in which the apically-directed cortical actin movements reversed direction such that the F-actin that had accumulated in the apical hemisphere began to move basally towards the emerging cleavage furrow (Roubinet et al., 2017).

Apically directed actin pulses polarize aPKC

Previously we showed that Par polarity proteins undergo complex cortical dynamics during neuroblast asymmetric cell division, and that Par cortical movements require an intact actin cytoskeleton (Oon and Prehoda, 2019). Examination of the cortical actin cytoskeleton revealed that it also highly dynamic (Figure 8 and Figure 8-Video 1), with key transitions in cortical movements at points in the cell cycle that are similar to those that occur in the protein polarity cycle. We determined the extent to which cortical actin and aPKC dynamics are correlated by simultaneously imaging GFP-aPKC expressed from its endogenous promoter with mRuby-Lifeact (Figure 9 and Figure 9-Video 1). We observed aPKC targeting to the apical membrane beginning approximately ten minutes before NEB, when small foci start to appear. The cortical pulses of actin that passed over these aPKC enrichments had no noticeable effect on them, suggesting that interphase cortical actin dynamics are not coupled to aPKC movement. Near NEB (e.g.

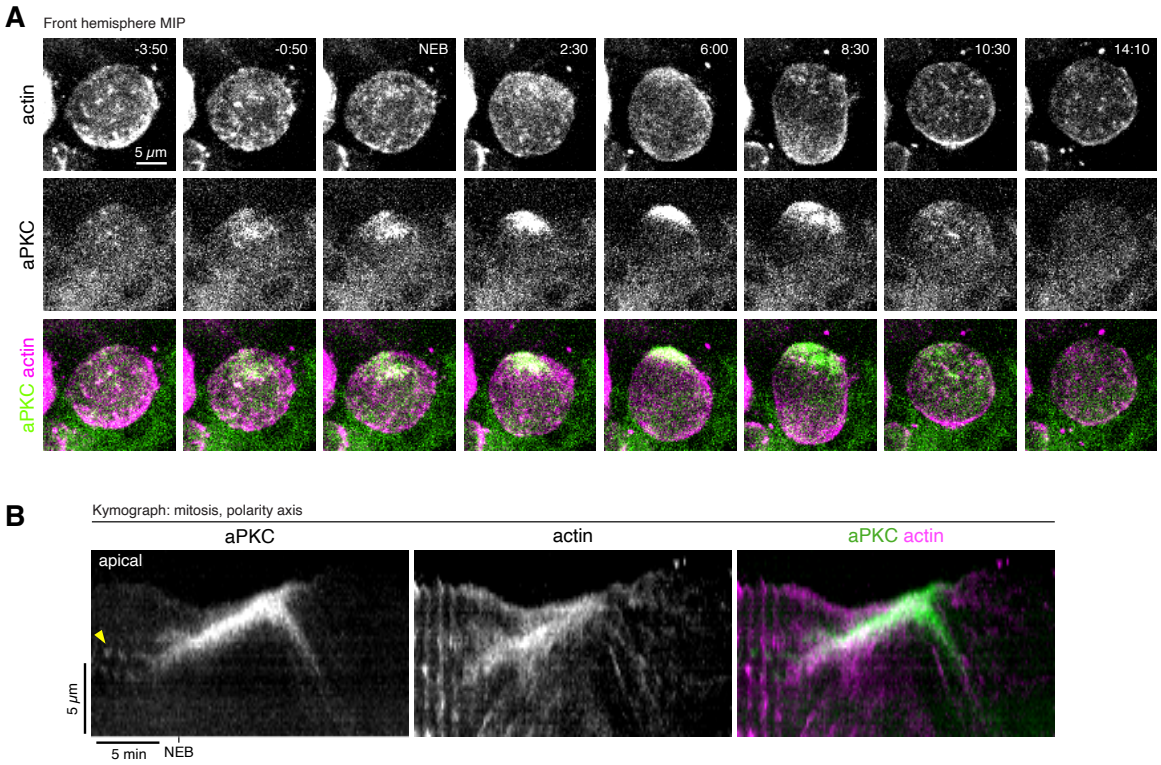

Figure 9 Coordinated actin and aPKC dynamics during the neuroblast polarity cycle. (A) Selected frames from Figure 9-Video 1 showing the correlated dynamics of aPKC and actin during polarization and depolarization. aPKC-GFP expressed from its endogenous promoter ("aPKC") and mRuby-LifeAct expressed via insc-GAL4/UAS ("actin") are shown via a maximum intensity projection (MIP) constructed from optical sections through the front hemisphere of the cell. **(B)** Kymograph made from a segment along the apical-basal axis of the neuroblast in Figure 9-Video 1 showing the correlated dynamics of aPKC and actin.

-0:50 in Figure 9-Video 1), the continued accumulation of aPKC lead to a diffusely scattered distribution over the apical hemisphere when the transition in actin cortical dynamics began. Continued accumulation led to a discontinuous distribution of aPKC in the apical hemisphere near NEB (e.g. -3:50 in Figure 9-Video 1). At this point, cortical actin pulses transitioned to the apically-directed phase. While interphase pulses had no apparent effect on cortical aPKC, aPKC began moving towards the apical pole when the apically-directed pulses began and these movements continued until it became fully polarized (2:30 in Figure 9-Video 1). Cortical actin pulses continued with no apparent

change in the polarized aPKC apical cap for several minutes (until approximately 6:00 in Figure 9-Video 1) when cortical actin and aPKC began simultaneously moving basally, toward the emerging cleavage furrow. Thus, cortical aPKC does not appear to be coupled to interphase actin pulses, but its movements are highly correlated with the apically-directed pulses that begin in early mitosis. Cortical actin pulses continue even after aPKC is fully polarized and both actin and aPKC simultaneously begin moving basally towards the cleavage furrow in anaphase.

Simultaneous imaging of aPKC and actin allowed us to examine precisely when disruption of the actin cytoskeleton influences aPKC dynamics (Figure 10 and Figure 10-videos 1-2). We introduced the actin depolymerizing drug Latrunculin A (LatA) at different phases of the cell cycle and examined how the movement of cortical aPKC was influenced as the cortical actin signal dissipated. We previously found that the actin cytoskeleton is required for the apically-directed polarizing movements of aPKC. Here we find that when cortical actin signal dissipates immediately before the targeting phase (Figure 10A,A' and Figure 10-video 1), aPKC is recruited to the apical cortex but rapidly depolarizes as apically targeted aPKC fails to coalesce and diffuses prematurely into the basal cortex. To determine if actomyosin dynamics is required for movement of aPKC, we treated prophase neuroblasts with Cytochalasin D (CytoD), an alternative actin polymerization inhibitor, and examine the movement of aPKC as actin dynamics are ablated. CytoD treatment disrupts cortical actin dynamics but permits a low amount of actin to localize to the cortex. When cortical actin fail to undergo apically-directed movements, aPKC continues to accumulate at the apical cortex, but fails to undergo coalescence (Figure 10B,B' and Figure 10-video 2). Similarly to LatA, CytoD treated

neuroblasts fail to retain aPKC at the apical domain as the remaining apical aPKC spreads into the basal cortex post-NEB. Thus, cortical actin and aPKC dynamics are highly correlated, and cortical aPKC movement is dependent on cortical actin, ceasing immediately following the loss of cortical actin.

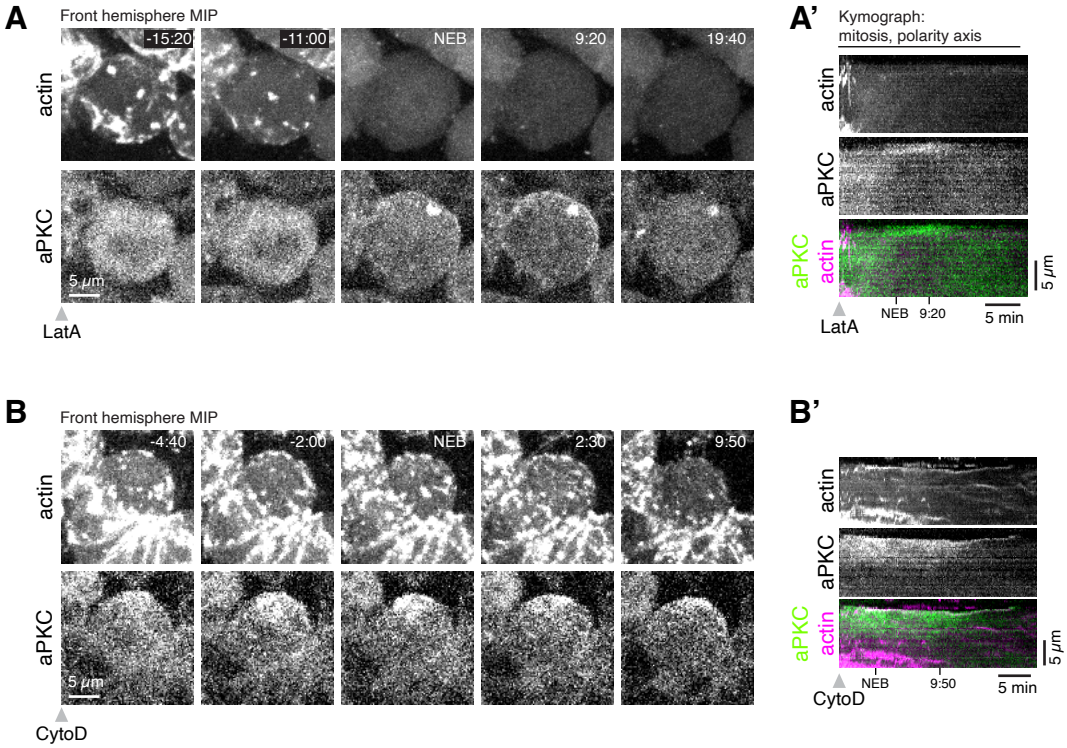

Figure 10 Effect of F-actin disruption on aPKC dynamics. (A) Selected frames from Figure 10-videos 1 showing how apically-directed aPKC movements cease upon complete loss of cortical actin. aPKC-GFP expressed from its endogenous promoter ("aPKC") and mRuby-LifeAct expressed via insc-GAL4/UAS ("actin") are shown via a maximum intensity projection (MIP) constructed from optical sections through the front hemisphere of the cell. **(A')** Kymograph made from Figure 10-video 1 using a section of each frame along the apical-basal axis. **(B)** Selected frames from Figure 10-video 2 as in (A) showing how apically-directed aPKC movements cease upon loss of cortical actin dynamics using a low dosage (50 μM) of cytochalasin D. **(B')** Kymograph made from Figure 10-video 2 using a section of each frame along the apical-basal axis.

Myosin II is a component of neuroblast cortical pulses

We observed morphological changes in interphase cells (Figure 8D and Figure 8-Video 1), and cortical aPKC movements that were correlated with cortical actin dynamics in early mitosis (Figure 9 and Figure 9-Video 1). These phenomena are consistent with force generation by the cortical actin pulses. While actin can generate force through polymerization, contractile forces are generated when it is paired with myosin II, and cortical pulsatile contractions of actomyosin have been observed in other systems (Michaux et al., 2018; Munro et al., 2004). Although there are numerous reports of myosin II dynamics in neuroblasts (Barros et al., 2003; Koe et al., 2018; Tsankova et al., 2017), no cortical pulses have been described and its localization has been described as uniformly cortical or cytoplasmic in interphase and before metaphase in mitosis. We used rapid imaging of the full cell volume, simultaneously following a GFP fusion of the myosin II regulatory light chain Spaghetti squash (GFP-Sqh) with mRuby-Lifeact, to determine if myosin II is part of the cortical actin pulses we observed. We found that myosin II is a component of every phase of the actin pulses (Figure 11 and Figure 11-Video 1), including the apically-directed pulses that polarize aPKC. Interestingly, however, while myosin II localized with actin and had very similar dynamics, the localization between the two was not absolute and there were often large cortical regions where the two did not colocalize in addition to the region where they overlapped (Figure 11 and Figure 11-Video 1). This is similar to the localization of the two proteins in the polarizing worm zygote (Michaux et al., 2018; Reymann et al., 2016). We also noticed that myosin II pulses were less persistent than their actin counterparts during the apically-directed phase of dynamics (Figure 11C). Thus, while there are some differences in the

dynamics of the two proteins, myosin II is a component of interphase and early mitotic neuroblast cortical pulses.

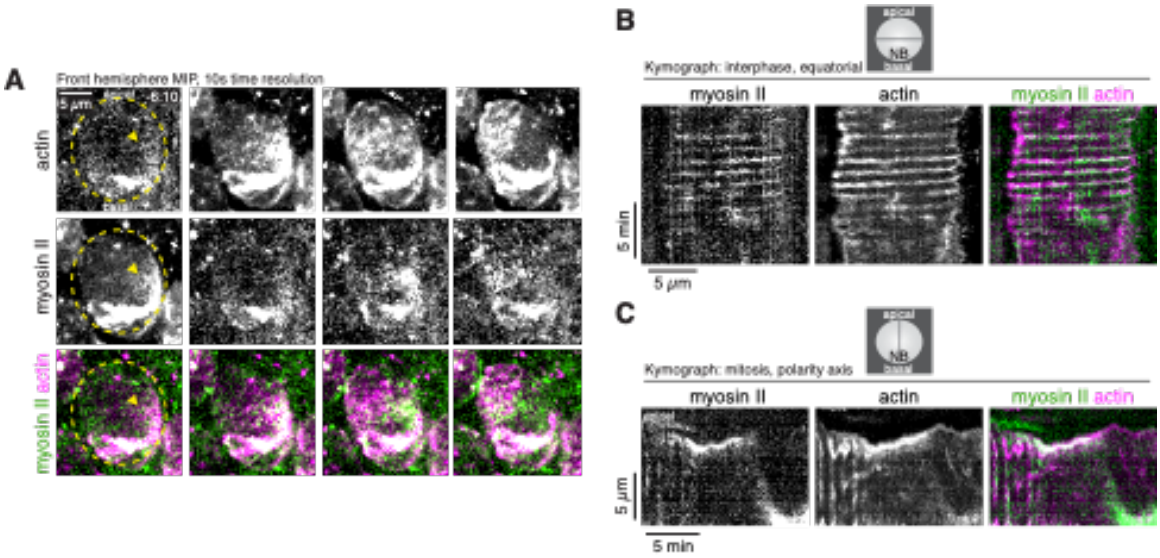

Figure 11 Dynamics of cortical actomyosin in asymmetrically dividing Drosophila larval brain neuroblasts. (A) Selected frames from Figure 11-Video 1 showing cortical actomyosin traveling across the equatorial face of the cell. GFP-Sqh expressed from its endogenous promoter ("Myosin II") and mRuby-LifeAct expressed via worniu-GAL4/UAS ("actin") are shown via a maximum intensity projection (MIP) constructed from optical sections through the front hemisphere of the cell. The outline of the neuroblast is shown by a dashed yellow line and arrowheads indicate the starting position of the cortical patches. Time is relative to nuclear envelope breakdown. **(B)** Kymograph constructed from frames of Figure 11-Video 1 during interphase using sections through the equatorial region of the cell as indicated. **(C)** Kymograph constructed from frames of Figure 11-Video 1 during mitosis using sections along the polarity axis of the cell as indicated.

A role for actomyosin pulsatile contractions in the initiation and maintenance of apical Par polarity in neuroblasts

Our results reveal previously unrecognized phases of pulsatile contractions during cycles of neuroblast asymmetric divisions. During interphase, transient cortical patches of actomyosin undergo highly dynamic movements in which they rapidly traverse the cell cortex, predominantly along the cell's equator, before dissipating and a new cycle begins

(Figure 11A). Shortly after mitotic entry the pulsatile movements reorient to align with the polarity axis. Importantly, the transition between these phases occurs shortly before the establishment of apical Par polarity, when discrete cortical patches of aPKC undergo coordinated movements towards the apical pole to form an apical cap (Figure 12). Pulsatile movements continue past metaphase when apical cap assembly is completed, suggesting that they may also be involved in cap maintenance.

While pulsatile behavior of actomyosin has not been reported during neuroblast polarization, it has been described for the apical constriction that occurs when epithelial cells delaminate undergo the transition to a neuroblast in the *Drosophila* embryo (An et al., 2017; Simões et al., 2017).

The actomyosin dynamics we have uncovered provide a framework for understanding how actomyosin participates in neuroblast apical polarity. First, apically directed pulsatile movements of actomyosin are consistent with the requirement for F-actin in the cortical flows that lead to coalescence of discrete aPKC patches (Figure 10) (Oon and Prehoda, 2019). Furthermore, the continuation of myosin II pulsatile movements after cap assembly is completed implies that they are also important for polarity maintenance (Figure 11). A role for actomyosin in cap maintenance would explain why the cap becomes dissociated when F-actin is depolymerized shortly after cap assembly (Oon and Prehoda, 2019). How might myosin II pulsatile contractions lead to the cortical flows we have observed during the polarization of the neuroblast apical cortex? Studies of worm zygote Par polarity provide a possible explanation. In this system, pulsatile contractions generate bulk cortical flows (i.e. advection) that lead to non-specific transport of cortically localized components (Goehring et al., 2011a;

Illukkumbura et al., 2019). Whether the cortical flows that occur during apical polarization of the neuroblast are also driven by advection will require further study.

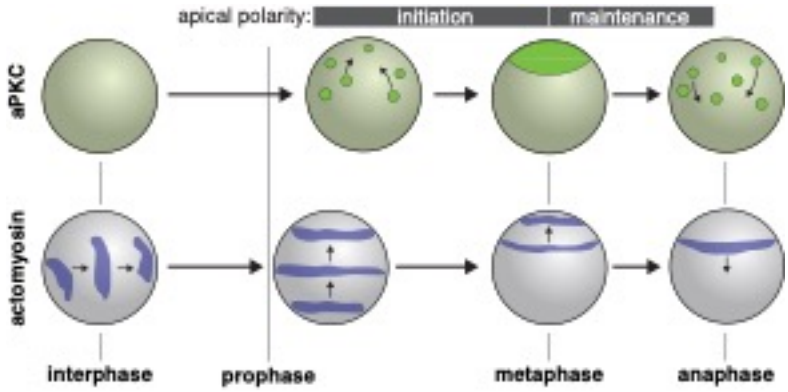

Figure 12 Model for role of actomyosin in neuroblast Par polarity. During interphase when aPKC is cytoplasmic, myosin II pulsatile contractions are predominantly equatorial. During apical polarity initiation in prophase and shortly before when discrete aPKC cortical patches begin to undergo coordinated movements towards the apical pole, myosin II pulsatile contractions reorient towards the apical cortex. Contractions are initially over a large surface area but become concentrated to the apical cortex as aPKC apical cap assembly is completed and the maintenance phase begins. At anaphase apical myosin II is cleared as it flows towards the cleavage furrow while the aPKC cap is disassembled.

MATERIALS AND METHODS

Fly strains and genetics

UAS-Lifeact-Ruby (Bloomington stock 35545), BAC-encoded aPKC-GFP (Besson et al., 2015) and Sqh-GFP (Royou et al., 2002) transgenes were used to assess F-actin, aPKC and myosin II dynamics, respectively. Expression of Lifeact was specifically driven in nerve cells upon crossing UAS-Lifeact-Ruby to insc-Gal4 (1407-Gal4, Bloomington stock 8751) or to wor-Gal4 (Bloomington stock 56553). The following genotypes were examined through dual channel live imaging: BAC-aPKC-GFP/Y ; insc-Gal4, UAS-Lifeact-Ruby/+ and ; worGal4, Sqh-GFP, UAS-Lifeact-Ruby/+ ;.

Live imaging

Third instar larvae were incubated in 30˚C overnight (~12 hours) prior to imaging and were dissected to isolate the brain lobes and ventral nerve cord, which were placed in Schneider's Insect media (SIM). Larval brain explants were placed in lysine-coated 35 mm cover slip dishes (WPI) containing modified minimal hemolymph-like solution (HL3.1). Explants were imaged on a Nikon Ti2 microscope equipped with a Yokogawa CSU-W1 spinning disk that was configured to two identical Photometrics Prime BSI Scientific CMOS cameras for simultaneous dual channel live imaging. Using the 1.2 NA Plan Apo VC water immersion objective, explants were magnified at 60x for visualization. Explants expressing Lifeact-Ruby, aPKC-GFP and Sqh-GFP were illuminated with 488 nm and 561 nm laser light throughout approximately 41 optical sections with step size of 0.5 μm and time interval of 10 seconds.

Image processing, analysis and visualization

Movies were analyzed in ImageJ (using the FIJI package) and in Imaris (Bitplane). Neuroblasts whose apical-basal polarity axis is positioned parallel to the imaging plane were cropped out to generate representative images and movies. Cortical edge and central maximum intensity projections (MIP) were derived from optical slices capturing the surface and center of the cell, respectively. Cortical MIPs were also used to perform kymograph analysis, where the change in localization profile of fluorescently-tagged fusion proteins within a 3 to 5 pixels wide region was examined across time. To track cortical movements over the length of the apical-basal axis, a vertical region parallel to the polarity axis was specified for the kymograph analysis. Similarly, a horizontal line orthogonal to the polarity axis that is superimposing on the presumptive equator was

specified for examining equatorial motions. Optical sections capturing the whole of the cell were assembled for 3D rendering and visualization in FIJI or Imaris. These volumetric reconstructions were then used to determine the timing of cortical motions characterized in this paper.

VIDEO LEGENDS

Figure 8-Video 1 Actin dynamics in a larval brain neuroblast.
The mRuby-Lifeact sensor expressed from the UAS promoter and *insc-GAL4* (drives expression in neuroblasts and progeny) is shown with a maximum intensity projection of the front hemisphere of the cell.

Figure 9-Video 1 Correlated dynamics of the Par protein aPKC and Actin in a larval brain neuroblast.
GFP-aPKC expressed from its endogenous promoter and the mRuby-Lifeact sensor expressed from the UAS promoter and *insc-GAL4* (drives expression in neuroblasts and progeny) are shown from simultaneously acquired optical sections with a maximum intensity projection of the front hemisphere of the cell.

Figure 10-video 1 Correlated dynamics of the Par protein aPKC and Actin in a larval brain neuroblast treated with Latrunculin A before mitosis.
GFP-aPKC expressed from its endogenous promoter and the mRuby-Lifeact sensor expressed from the UAS promoter and *insc-GAL4* (drives expression in neuroblasts and progeny) are shown from simultaneously acquired optical sections with a maximum

intensity projection of the front hemisphere of the cell. LatA was added to the media surrounding the larval brain explant at the indicated time.

Figure 10-video 2 Correlated dynamics of the Par protein aPKC and Actin in a larval brain neuroblast treated with Cytochalasin D during prophase.
GFP-aPKC expressed from its endogenous promoter and the mRuby-Lifeact sensor expressed from the UAS promoter and *insc-GAL4* (drives expression in neuroblasts and progeny) are shown from simultaneously acquired optical sections with a maximum intensity projection of the front hemisphere of the cell. CytoD was added to the media surrounding the larval brain explant at 2 minutes prior to the beginning of the movie.

Figure 11-Video 1 Correlated dynamics of myosin II and Actin in a larval brain neuroblast.
GFP-Sqh (the myosin II regulatory light chain, Spaghetti Squash) expressed from its endogenous promoter and the mRuby-Lifeact sensor expressed from the UAS promoter and *worniu-GAL4* (drives expression in neuroblasts and progeny) are shown from simultaneously acquired optical sections with a maximum intensity projection of the front hemisphere of the cell and the medial optical section. The neuroblast is highlighted by a dashed circle.

CHAPTER IV

ROLE OF ACTOMYOSIN IN CORTICAL POLARITY: A COMPARISON BETWEEN TWO WELL-ESTABLISHED POLARITY MODELS

^ This chapter contains unpublished co-authored material.

C.H. Oon and K.E. Prehoda

Institute of Molecular Biology, Department of Chemistry and Biochemistry
1229 University of Oregon, Eugene OR 97403

Author Contributions: C.H. Oon contributed to Conceptualization, Writing—original draft, Writing—review and editing. K.E. Prehoda contributed to Conceptualization, Writing—original draft, Writing—review and editing.

SUMMARY

Using full volume, rapid live imaging technique, we demonstrated that Par polarization in neuroblasts is a dynamic, multistep process that requires actomyosin (Oon & Prehoda, 2019). Starting at interphase, F-actin and contractile myosin II exhibit highly dynamic, non-deterministic pulsatile waves that turnover rapidly (in a timescale of seconds) and appear indiscriminately in both the apical and basal cortex. While movement of these pulsatile waves can be randomly oriented and sporadic, appearance of the pulses is associated with deformation in the corresponding section of the cell

membrane–a characteristic viscoelastic behavior of the tensioned cortex. In early prophase, cytoplasmic Par protein complex is asymmetrically targeted to discrete, bright foci at the apical cortex–where they continue to accumulate into larger, higher intensity apical patches. At this stage, Par protein dynamics are not coupled to actomyosin dynamics since discrete apical Par patches remain relatively static and their spatial distribution appears to be unaffected by the unoriented interphase pulses. Interphase pulses cease at approximately 3 minutes prior to nuclear envelope breakdown (NEB) as the neuroblast initiates assembly of a sparsely distributed apical actomyosin network. Following its appearance, this nascent actomyosin network contracts apically to form a highly-tensioned, dense network at the apical pole. Meanwhile, discrete apical Par patches move apically in a coordinated manner to coalesce into a single, continuous apical cap at the apical pole–marking the previously recognized apical Par polarized state. Both timing and movement of apically-directed cortical flow coincide with that of Par patches during coalescence. Notably, the dense actomyosin network and the apical Par protein cap also appear to colocalize at the apical pole.

The apical Par protein cap is maintained until anaphase onset, when Par proteins begin depolarizing towards the basal cortex. Correspondingly, the filamentous myosin II continues to undergo apically-directed contractions upon formation of the apical cap, although its localization and activity decrease as a function of time after cap formation. F-actin, on the other hand, remains organized in a dense apical network until anaphase onset, during which it dissociates and undergoes basally-directed cortical flow. Considering that both the spatial distribution and speed of cortical Par proteins are tightly correlated with that of actomyosin from the onset of coalescence through the end of

depolarization, these results suggest that Par complex and actomyosin dynamics become spatiotemporally linked during Par polarization. Accordingly, asymmetric foci targeting, patch growth, coalescence, and maintenance of Par polarity require an intact F-actin network. Pharmacologically ablating F-actin or its dynamics reduces the amount of cytoplasmic Par proteins loaded onto the apical cortex and prevents coordinated movement of apical Par patches during coalescence–ultimately leading to ectopic spreading of apical Par proteins and premature depolarization. These results support a model where gradients in actomyosin contractility produces apically-directed cortical flow that helps Par proteins reach the threshold required to transition from a low concentration state (i.e. the discrete and sparsely distributed Par foci/patches at the apical hemisphere) to a highly-concentrated state (i.e. the densely-populated apical cap at the apical pole) during coalescence. After which, mechanical tension of the F-actin network keeps Par proteins in a polarized state until the onset of depolarization.

DISCUSSION

Par proteins are subjected to random movements

At the molecular scale, cortically associated Par proteins are known to exhibit non-directional random motions such as diffusion (i.e. Brownian motion) and cortical-cytoplasmic association and dissociation in the one-cell stage *C. elegans* embryos (Cheeks *et al.*, 2004; Goehring *et al.*, 2011a; Robin *et al.*, 2014). Both diffusion and cortical-cytoplasmic exchange are thermodynamically favorable and spontaneously occurring since they tend to create a disperse, less ordered state. This randomly mobile behavior of Par proteins may potentially pose as an energetically costly barrier for pattern formation given that patterning increases order (i.e. decrease entropy). How then do cells

overcome this thermodynamic barrier to achieve spatial organization? Or more specifically with regards to cortical polarity, how do polarizing cells transition from a spontaneously random distribution to a patterned distribution–that is transiently stable during polarization–while cortical proteins that need to be spatially organized are also subjected to random movements? Hence polarizing systems need to account for random motions of cortical proteins during pattern formation. As we will discuss in the following sections, *C. elegans* embryos and *Drosophila* neuroblasts employ additional mechanisms to overcome these entropic forces in order to create and maintain cortical patterns.

Cortical flow polarizes the Par complex in worm embryos and fly neuroblasts

Cortical pattern formation is tied to the actomyosin cytoskeletal network to a great extent in both worm embryos and fly neuroblasts. In worm embryos, asymmetric contraction of actomyosin generates anteriorly directed cortical flow that breaks the symmetrical distribution of the Par complex. In fly neuroblasts, apically-direct cortical flow drives coalescence of individually clustered Par proteins into a single unity at the apical pole during polarization. In both systems, Par proteins must travel against the concentration gradient in order to become enriched in the Par domain–another thermodynamically unfavorable process that involves transitioning from a sparsely distributed, lower concentration state to a densely populated, higher concentration state (which also decreases entropy). Considering that large scale flow of the actomyosin cortex is spatiotemporally correlated with long range displacement of the Par complex during polarization of both model systems, a conserved model where polarizing cells mobilize the mechanically active actomyosin cortex to facilitate continuous recruitment of Par proteins into the Par domain and to achieve a stable polarized state is proposed.

Upon ATP hydrolysis, myosin II motor converts chemical energy into mechanical force to power bulk flow of the actomyosin cortex which mobilizes the entrained Par polarity complex. Cortical flow travels in a direction that goes against the concentration gradient of Par proteins, thereby enabling Par proteins to assemble at the Par domain. In this model, actomyosin-dependent mechanochemical reaction helps overcome random entropic motions as well as the Par concentration gradient in order to generate Par polarity.

How does cortical flow move Par proteins across the cortex during polarization? The worm embryos may provide additional clues to address this question. Since Par proteins and actomyosin display partial colocalization during cortical flow in worm embryos, it is speculated that actomyosin acts through passive advective transport to promote long range displacement of cortical proteins. If actomyosin is fluid, then Par proteins that are embedded within the fluid network are subjected to bulk motion of the corresponding network. Advective transport can be quantified by the Péclet number ($P_e = Lu/D$), where longer distances L, higher flow velocity u, and/or, lower diffusion coefficient D can promote a regime where $P_e > 1$ and advection dominates diffusion to become the predominant mode for motion. $P_e \approx 2.5$ has been reported for Par-6 in worm embryos (Goehring *et al.*, 2011a), suggesting that fluid flow rate u and/or hydrodynamic distance L are sufficiently large to combat Brownian motion of Par-6 and to facilitate its directional transport. Consistently, biophysical study recapitulated segregation profile of Par-6–that is comparable to the *in vivo* data–when their modeling incorporated advection as the sole parameter that accounts for directional movement and other non-directional parameters such as diffusion and membrane-cytoplasmic exchange (Goehring *et al.*,

2011a). Mathematical modeling indicates that advection is sufficient to power long range displacement and segregation of the Par complex. Hence anteriorly-directed cortical flow is thought to advect Par complex anteriorly to establish polarity in the one-cell staged worm embryo. Although apical Par proteins and actomyosin also partially colocalize in the polarizing neuroblasts, whether advection triggers coalescence of Par patches has not been tested in neuroblasts.

Two distinct mechanisms for Par polarity maintenance

Considering that cortical Par complex are subjected to random diffusion and exchange between cortical and cytoplasmic pool, polarized Par proteins likely exist in a dynamic steady state during polarity maintenance–when mobile Par proteins remain stably accumulated in the Par domain. Random movements will likely prevent continuous enrichment of the Par complex in their corresponding domains and cause dispersal, if Par proteins are not subjected to additional influence (i.e. advective transport). Hence to maintain a net-accumulation of mobile Par proteins, polarized cells need to employ additional mechanism to fight dispersion. In worm embryos, actomyosin contractility and cortical flow subside during maintenance phase as mutual inhibition via reciprocal phosphorylation of anterior and posterior Par proteins take over as the primary mechanism to maintain polarity. (Etemad-Moghadam *et al.*, 1995; Tabuse *et al.*, 1998; Cuenca *et al.*, 2003). During polarity maintenance, anterior and posterior Par proteins exist in a concentration gradient, where their concentration is highest in their respective domain and lowest in their opposite domain and where there is a gradual decrease in their corresponding concentrations approaching the boundary of their respective domains (Goehring *et al.*, 2011b). Thus, anterior and posterior Par proteins freely diffuse across

their domain boundary, but mutual phosphorylation between the two Par protein groups keeps them asymmetrically segregated.

While contractility ceases upon polarity establishment in worm embryos, in fly neuroblasts myosin II remains mechanically active upon coalescence (although at decreasing levels) and tensioned F-actin network remains densely populated at the apical pole. Persistence of F-actin network until the onset of depolarization despite attenuation of myosin II contractions following coalescence implies that myosin II and F-actin may play distinct roles to polarize the Par complex: myosin II driven cortical flow helps segregate Par complex to the apical pole during polarity establishment while F-actin retains apically-targeted Par proteins during both establishment and maintenance. Consistently, in metaphase neuroblast treated with actin depolymerizer at a time when myosin II activity has subsided, apical Par protein cap fragments into several, discontinuous clusters before spreading into the basal cortex (Oon & Prehoda, 2019), suggesting than an intact, cortical F-actin network is essential for Par polarity maintenance. Moreover, prophase treated neuroblasts display partial asymmetric targeting phenotype where Par proteins were apically-targeted at reduce levels before spreading into the basal cortex. Thus pharmacological ablation experiments support the role of F-actin in retaining cortically targeted Par complex at its designated domain during polarity establishment and maintenance. They suggest a model where myosin II contractility facilitates coalescence while F-actin enables retention of asymmetrically targeted Par proteins during Par polarization.

How might F-actin retain mobile Par proteins within the Par domain? Increase contractility at the apical pole is associated with a denser, apical F-actin network,

implicating that active tension exerted onto F-actin causes an increase in its network density and viscosity. This increase in total mechanical tension may allow F-actin to reduce long range diffusion (and other random movements) by exerting viscous drag on the entrained Par proteins, thereby limiting their mobility and cortical dissociation. Accordingly, F-actin plays a similar role during polarity establishment of the worm embryo as viscosity of the cytoskeletal meshwork is one of the two key prerequisites for cortical flow (Mayer *et al.*, 2010), presumably by limiting diffusion. Thus F-actin serves as a scaffold that retains cortically targeted proteins by modulating their movements through mechanical tension.

Cortical Par complex exchanges between diffuse and clustered forms

Aside from cortical flow, the two polarity models also exhibit another similarity: Par complex exists in diffuse and clustered assemblies during polarization. In neuroblasts, diffuse Par proteins accumulate into apical Par patches before undergoing apically-directed flow (Oon and Prehoda, 2019). In worm embryos, Par-6/aPKC also exists in both diffuse and clustered forms, specifically where clustered Par-6/aPKC tend to colocalize with membrane-associated Par-3 while diffuse Par-6/aPKC tend to colocalize with membrane-associated RhoGTPase Cdc42 (Wang *et al.*, 2017). What could be the purpose of having two distinct pools of Par proteins? Single cell biochemical approach in worm embryos demonstrated that Par-3/Par-6/aPKC forms larger oligomeric complex during polarity establishment and oligomerization decreases during maintenance (Dickinson *et al.*, 2017). Notably, increase in Par oligomeric state is associated with increase in membrane association and decrease in diffusion. P_e is also positively correlated with Par-3 oligomerization in single particle tracking, thus implicating that

clustering makes Par proteins more amenable to bulk flow. Consistently, monomeric, membrane-associated Par-3 retains the ability to recruit Par-6 and aPKC, but they fail to become segregated by cortical flow (Rodriguez *et al.*, 2017). Further genetic analysis and pharmacological inhibition experiments demonstrated that Par-3 oligomerization promotes recruitment of active Par-6/aPKC into inactive clusters, while membrane targeted Cdc42 and its associated activity competes with Par-3 to promote recruitment of oligomerized, inactive Par-6/aPKC into an active diffuse pool (Rodriguez *et al.*, 2017; Wang *et al.*, 2017).

These results support a model where Par-3 associated cluster is receptive to the segregation cue while Cdc42 associated diffuse pool permits Par complex to carry out its function via aPKC activity. However, why active Cdc42 fails to directly recruit active Par-6/aPKC remains unclear (Munro, 2017). Nevertheless, this model is consistent with the spatiotemporal distribution profile of the Par complex in worm embryos, where clustering of Par-3 and its colocalization with Par-6/aPKC are predominantly seen in polarity establishment–when segregation via cortical flow takes place–while colocalization of diffuse Cdc42 and unclustered Par-6/aPKC occurs more frequently in maintenance–when aPKC activity plays a critical role in mutual inhibition of posterior Par to maintain polarity (Rodriguez *et al.*, 2017; Wang *et al.*, 2017; Dickinson *et al.*, 2017). This could also explain for why neuroblasts undergo an additional cortical flow step during polarization, despite achieving asymmetrical distribution of diffuse, active Par complex upon asymmetric targeting (Oon and Prehoda, 2019; Lafoya and Prehoda, 2021). Because Par proteins become subjected to cortical flow after arriving at a more accumulated state (i.e. apical Par patches) in fly neuroblasts, it is probable that clustering

also makes Par complex more responsive to bulk flow in this system. Hence switching between diffuse and clustered form may account for how the Par complex acquire and maintain a polarized distribution while retaining the ability to polarize downstream substrates.

Role of actomyosin in neuroblast basal polarity

Cortical actomyosin is also known to be required for polarization of basal factors (Knoblich *et al.*, 1995; Knoblich *et al.*, 1997; Broadus & Doe, 1997; Shen *et al.*, 1998; Barros *et al.*, 2003; Erben *et* al., 2008; Hannaford *et al.*, 2018). In neuroblasts expressing sqh^{1}, myosin II heavy chain forms inactive aggregates while basal fate determinants–Mira, Pros, and Numb–either delocalize from the basal cortex and ectopically localize to the mitotic spindle, become symmetrically cortical, or become cytoplasmic–depending on the severity of the phenotype that the mutant neuroblasts display (Barros *et al.*, 2003). Suppressing myosin II activity with Y-27632 mediated drug inhibition causes myosin II to become cytoplasmic and basal factors to become symmetrically cortical (Barros *et al.*, 2003; Erben *et* al., 2008; Hannaford *et al.*, 2018). The variation in basal polarity phenotypes between sqh^{1} hypomorph and Y-27632 inhibition has been attributed to differences in F-actin localization (Barros *et al.*, 2003). F-actin becomes fragmented and discontinuous in sqh^{1} hypomorphs and consequently produces a more severe cortical targeting phenotype. In contrast, F-actin remains cortical and intact in majority of the Y-27632 treated neuroblasts, thereby permitting basal proteins to remain membrane associated–even though they fail to become asymmetrically segregated. This interpretation suggests that F-actin and myosin II play distinct roles in mediating basal polarity, where F-actin is responsible for cortical targeting of basal proteins while myosin

II activity facilitates asymmetrical distribution of basal factors. Accordingly, experiments in cultured neuroblasts treated with chemical inhibitors of F-actin showed that virtually eliminating F-actin from the entire cell cortex causes basal determinants Pros and Stau to delocalize from the basal cortex and to become redistributed to the cytoplasm (Broadus & Doe, 1997).

While earlier genetic and pharmacological inhibition studies have demonstrated an essential role for actomyosin in basal protein localization, how actomyosin works in concert with Par complex to dynamically regulate the spatiotemporal distribution of basal factors remains unclear. Considering that myosin II and basal proteins localize to mutually exclusive domains when basal factors are polarized–from prophase through the end of metaphase–and that basal factors fail to polarize when myosin II activity is disrupted, it is proposed that myosin II exclude basal proteins from the apical cortex to generate basal asymmetry (Barros *et al.*, 2003). Alternatively, a model where Par complex and actomyosin are sequentially involved in basal polarity has been proposed: aPKC kinase activity is critical for initial segregation of basal factor Mira prior to nuclear envelope breakdown (NEB) while actomyosin activity is essential to maintain asymmetry of basal factor post-NEB (Hannaford *et al.*, 2018). Both models insinuate that myosin Il activity acts immediately upstream of basal polarity. However, the finding that myosin II contractility is spatiotemporally linked to apical Par polarity proteins during polarization suggests that contractility may act indirectly and upstream of the Par complex to promote establishment and maintenance of basal polarity. In this model, apically-directed cortical flow generated by gradients of myosin II contractility establishes Par polarity. Following which, aPKC activity functions to establish and maintain basal polarity pre- and post-

NEB. Accordingly, cortical targeting of Mira relies on its basic, hydrophobic motif throughout the polarization cycle (Hannaford *et al.*, 2018), implicating that phosphorylation of its membrane binding sites may serve as the primary regulatory mechanism modulating Mira distribution during basal polarity establishment and maintenance. This third model would suggest a conserved role for the Par complex in maintaining polarity, given that aPKC activity also functions to maintain previously established asymmetry in *C. elegans* embryo (Hurov *et al.*, 2004; Hao *et al.*, 2006; Beatty *et al.*, 2010; Motegi *et al.*, 2011).

Although active tension generated from myosin II contraction is less likely to be directly involved in maintaining basal polarity, mechanical tension of F-actin may still play a direct role in limiting mobility of basal proteins during polarization. FRAP experiments showed that fluorescence recovery of cortical Mira in mitosis occurs approximately half as quickly as in interphase (Hannaford *et al.*, 2018), suggesting that neuroblasts employ additional mechanism to reduce mobility of Mira (i.e. either through lateral diffusion and/or membrane-cytoplasmic exchange) during mitosis. Specifically, this kinetic behavior implies that Mira exists in a dynamic equilibrium state during polarity maintenance, where there are mechanisms in place to fight dispersal and to maintain a net accumulated state of the randomly diffusing Mira at the basal cortex. Similarly to apical polarity maintenance, F-actin density may provide mechanical tension by exerting viscous drag on basal proteins to limit their long range diffusion and to maintain basal polarity.

CONCLUDING REMARKS

Prior to the work done in this dissertation, Par polarity establishment and maintenance are thought to occur via two distinct mechanisms in different polarity models, with cortical flow driving polarization in *C. elegans* embryos and asymmetrical targeting facilitating polarization in *Drosophila* neuroblasts. Through a series of live imaging experiments in neuroblasts, Par complex dynamics reveal to us that Par polarization is highly dynamic and occurs via asymmetric targeting and coalescence in this system. In addition, neuroblast actomyosin dynamics show that coalescence is spatiotemporally linked to cortical flow, implicating that cortical flow is a conserved mechanism for initial symmetry breaking of the Par complex during Par polarity establishment. Along with actomyosin dynamics, pharmacological inhibition experiments reveal a conserved role for F-actin in retaining cortically targeted proteins.

APPENDIX

APPENDIX A: SUPPLEMENTAL MATERIAL FOR CHAPTER II

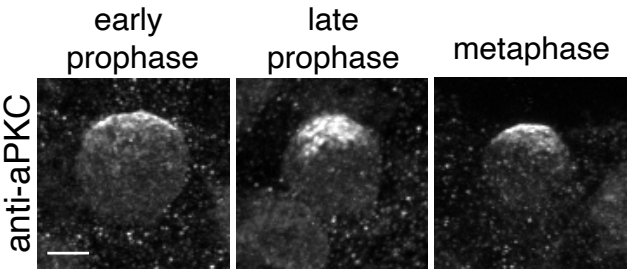

Figure 1–supplement 1 Cortical localization in fixed neuroblasts. Localization of aPKC in fixed neuroblasts. Cortical patches of aPKC are present in 12 μm maximum intensity projections of three different wild type neuroblasts stained with an anti-aPKC antibody. Cell cycle phases are from DAPI staining (early prophase, late prophase, metaphase; not shown). Scale bar is 5 μm.

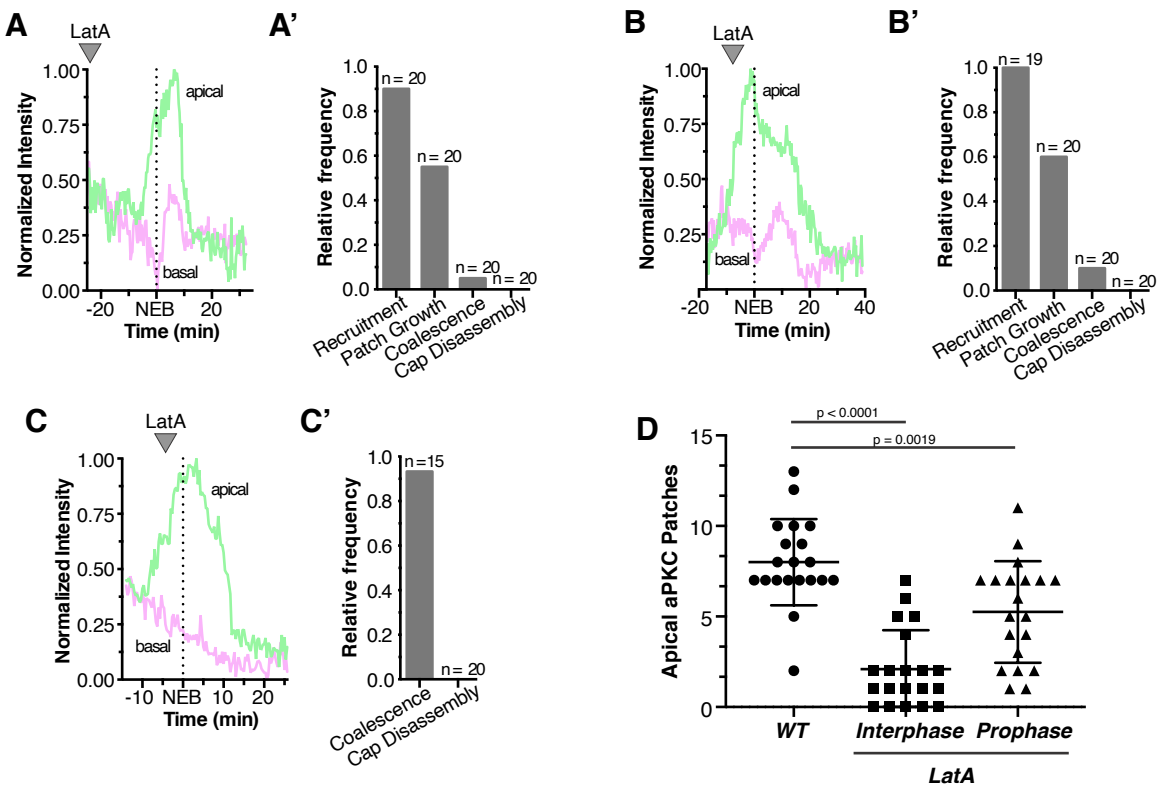

Figure 4–supplement 1 Quantification of Latrunculin A effects on aPKC localization dynamics (A) Effect of treating an interphase neuroblast with LatA on aPKC localization. Normalized apical and basal cortical intensity is shown from Figure 4-video 1. **(A')** The frequency of neuroblasts treated with LatA in interphase that exhibit any aPKC recruitment to the cortex ("Recruitment"), growth of foci into patches ("Patch Growth"), coalescence of patches into an apical cap ("Coalescence"), and cap disassembly, are shown. Frequency is relative to wild type neuroblasts (wild type neuroblasts exhibit each effect with a frequency of 1.0; n = 20). **(B)** Effect of treating a neuroblast with LatA following the initial cortical recruitment events on normalized apical and basal cortical aPKC intensity (from Figure 4-video 2). **(B')** The frequency of neuroblasts treated with LatA following the initial cortical recruitment events that exhibit characteristics of the neuroblast polarity cycle, as in panel A'. **(C)** Effect of treating a neuroblast with LatA near cap coalescence on normalized apical and basal cortical aPKC intensity (from Figure 4-video 3). **(C')** The frequency of neuroblasts treated with LatA near cap coalescence that exhibit characteristics of the neuroblast polarity cycle, as in panel A' ("Recruitment" and "Patch Growth" phases are not shown because they are completed by metaphase). **(D)** Number of apical aPKC patches in wild type neuroblasts and those treated with LatA either in interphase or prophase. Error bars represent one standard deviation from the mean. Statistical significance was calculated using a two-tailed t-test. Data are included in Figure 4-supplement 1 source data 1.

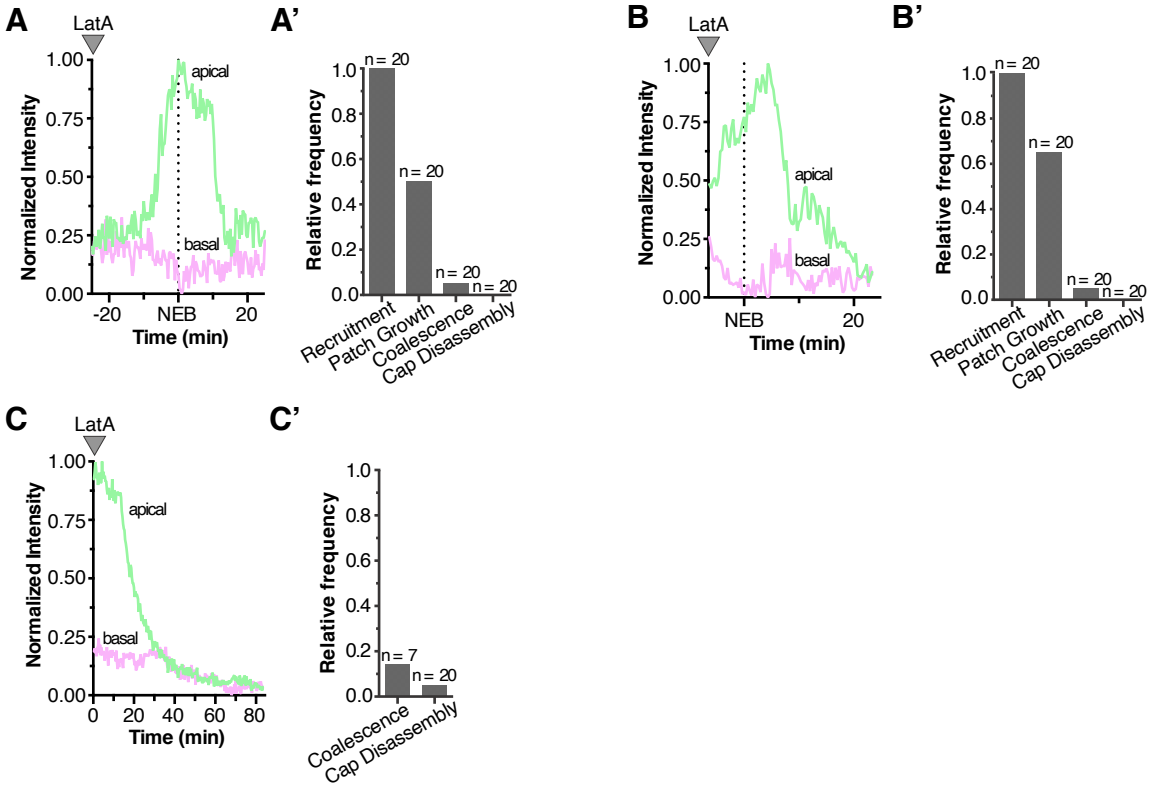

Figure 6–supplement 1 Quantification of Latrunculin A effects on Baz localization dynamics (A) Effect of treating an interphase neuroblast with LatA on Baz localization. Normalized apical and basal cortical intensity is shown from Figure 6-video 1. **(A')** The frequency of neuroblasts treated with LatA in interphase that exhibit any Baz recruitment to the cortex ("Recruitment"), growth of foci into patches ("Patch Growth"), coalescence of patches into an apical cap ("Coalescence"), and cap disassembly, are shown. Frequency is relative to wild type neuroblasts. **(B)** Effect of treating a neuroblast with LatA following the initial cortical recruitment events on normalized apical and basal cortical Baz intensity (from Figure 6-video 2). **(B')** The frequency of neuroblasts treated with LatA following the initial cortical recruitment events that exhibit Baz cortical dynamics, as in panel A'. **(C)** Effect of treating a neuroblast with LatA following cap coalescence on normalized apical and basal cortical Baz intensity (from Figure 6-video 3). **(C')** The frequency of neuroblasts treated with LatA following cap coalescence that exhibit Baz cortical dynamics, as in panel A' ("Recruitment" and "Patch Growth" phases are not shown because they are completed by metaphase).

APPENDIX

APPENDIX B: SUPPLEMENTAL MATERIAL FOR CHAPTER III

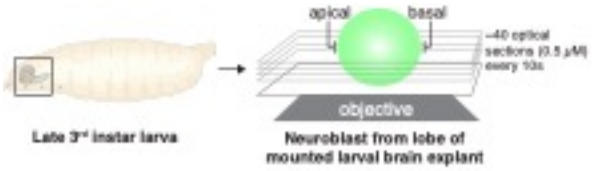

Figure 8 - figure supplement 1 Imaging and analysis scheme for rapid, full volume imaging of Drosophila neuroblasts from larval brain explants. Larval brains from 3rd instar larvae were mounted and imaged along the neuroblast polarity axis ("apical" and "basal"). Optical sections across the full cell volume were acquired every 10 seconds and used to construct maximum intensity projections.

REFERENCES CITED

Abeysundara N, Simmonds AJ, Hughes SC. 2018. Moesin is involved in polarity maintenance and cortical remodeling during asymmetric cell division. *Mol Biol Cell* **29**:419–434. doi:10.1091/mbc.E17-05-0294

Albertson R, Doe CQ. 2003. Dlg, Scrib and Lgl regulate neuroblast cell size and mitotic spindle asymmetry. *Nat Cell Biol* **5**:166–170. doi:10.1038/ncb922

An Y, Xue G, Shaobo Y, Mingxi D, Zhou X, Yu W, Ishibashi T, Zhang L, Yan Y. 2017. Apical constriction is driven by a pulsatile apical myosin network in delaminating Drosophila neuroblasts. *Dev Camb Engl* **144**:2153–2164. doi:10.1242/dev.150763

Atwood SX, Prehoda KE. 2009. aPKC phosphorylates Miranda to polarize fate determinants during neuroblast asymmetric cell division. *Curr Biol* **19**:723–729. doi:10.1016/j.cub.2009.03.056

Bailey MJ, Prehoda KE. 2015. Establishment of Par-Polarized Cortical Domains via Phosphoregulated Membrane Motifs. *Dev Cell* **35**:199–210. doi:10.1016/j.devcel.2015.09.016

Barros CS, Phelps CB, Brand AH. 2003. Drosophila nonmuscle myosin II promotes the asymmetric segregation of cell fate determinants by cortical exclusion rather than active transport. *Dev Cell* **5**:829–840.

Beatty A, Morton D, Kemphues K. 2010. The C. elegans homolog of Drosophila Lethal giant larvae functions redundantly with PAR-2 to maintain polarity in the early embryo. *Development* **137**:3995-4004. doi: 10.1242/dev.056028

Bello B, Reichert H, Hirth F. 2006. The brain tumor gene negatively regulates neural progenitor cell proliferation in the larval central brain of Drosophila. *Development* **133**:2639-2648. doi: 10.1242/dev.02429

Besson C, Bernard F, Corson F, Rouault H, Reynaud E, Keder A, Mazouni K, Schweisguth F. 2015. Planar Cell Polarity Breaks the Symmetry of PAR Protein Distribution prior to Mitosis in Drosophila Sensory Organ Precursor Cells. *Curr Biol CB* **25**:1104–1110. doi:10.1016/j.cub.2015.02.073

Betschinger J, Mechtler K, Knoblich JA. 2003. The Par complex directs asymmetric cell division by phosphorylating the cytoskeletal protein Lgl. *Nature* **422**:326–330. doi:10.1038/nature01486

Betschinger J, Knoblich JA. 2004. Dare to be different: asymmetric cell division in Drosophila, C. elegans and vertebrates. *Curr Biol* **14**:R674-685. doi: 10.1016/j.cub.2004.08.017

Betschinger J, Mechtler K, Knoblich JA. 2006. Asymmetric segregation of the tumor suppressor brat regulates self-renewal in Drosophila neural stem cells. *Cell* **124**:1241-1253. doi: 10.1016/j.cell.2006.01.038

Broadus J, Doe CQ. 1997. Extrinsic cues, intrinsic cues and microfilaments regulate asymmetric protein localization in Drosophila neuroblasts. *Curr Biol* **7**:827–835.

Buszczak M, Paterno S, Lighthouse D, Bachman J, Planck J, Owen S, Skora AD, Nystul TG, Ohlstein B, Allen A, Wilhelm JE, Murphy TD, Levis RW, Matunis E, Srivali N, Hoskins RA, Spradling AC. 2007. The carnegie protein trap library: a versatile tool for Drosophila developmental studies. *Genetics* **175**:1505–1531. doi:10.1534/genetics.106.065961

Cabernard C, Prehoda KE, Doe CQ. 2010. A spindle-independent cleavage furrow positioning pathway. *Nature* **467**:91–94. doi:10.1038/nature09334

Cai Y, Yu F, Lin S, Chia W, Yang X. 2003. Apical complex genes control mitotic spindle geometry and relative size of daughter cells in Drosophila neuroblast and pI asymmetric divisions. *Cell* **112**:51-62. doi: 10.1016/s0092-8674(02)01170-4

Cheeks RJ, Canman JC, Gabriel WN, Meyer N, Strome S, Goldstein B. 2004. C. elegans PAR proteins function by mobilizing and stabilizing asymmetrically localized protein complexes. *Curr Biol* **14**:851-862. doi: 10.1016/j.cub.2004.05.022

Choksi SP, Southall TD, Bossing T, Edoff K, de Wit E, Fischer BE, van Steensel B, Micklem G, Brand AH. 2006. Prospero acts as a binary switch between self-renewal and differentiation in Drosophila neural stem cells. *Dev Cell* **11**:775-789. doi: 10.1016/j.devcel.2006.09.015

Connell M, Cabernard C, Ricketson D, Doe CQ, Prehoda KE. 2011. Asymmetric cortical extension shifts cleavage furrow position in Drosophila neuroblasts. *Mol Biol Cell* **22**:4220–4226. doi:10.1091/mbc.E11-02-0173

Cuenca AA, Schetter A, Aceto D, Kemphues K, Seydoux G. 2003. Polarization of the C. elegans zygote proceeds via distinct establishment and maintenance phases. *Development* **130**:1255-1265. doi: 10.1242/dev.00284

Dickinson DJ, Schwager F, Pintard L, Gotta M, Goldstein B. 2017. A Single-Cell Biochemistry Approach Reveals PAR Complex Dynamics during Cell Polarization. *Dev Cell* **42**:416-434.e11. doi: 10.1016/j.devcel.2017.07.024

Doe CQ, Bowerman B. 2001. Asymmetric cell division: fly neuroblast meets worm zygote. *Curr Opin Cell Biol* **13**:68-75. doi: 10.1016/s0955-0674(00)00176-9

Erben V, Waldhuber M, Langer D, Fetka I, Jansen RP, Petritsch C. 2008. Asymmetric localization of the adaptor protein Miranda in neuroblasts is achieved by diffusion and sequential interaction of Myosin II and VI. *J Cell Sci* **121**:1403-1414. doi: 10.1242/jcs.020024

Etemad-Moghadam B, Guo S, Kemphues KJ. 1995. Asymmetrically distributed PAR-3 protein contributes to cell polarity and spindle alignment in early C. elegans embryos. *Cell* **83**:743-52. doi: 10.1016/0092-8674(95)90187-6

Goehring NW, Trong PK, Bois JS, Chowdhury D, Nicola EM, Hyman AA, Grill SW. 2011. Polarization of PAR proteins by advective triggering of a pattern-forming system. *Science* **334**:1137–1141. doi:10.1126/science.1208619

Goehring NW, Hoege C, Grill SW, Hyman AA. 2011. PAR proteins diffuse freely across the anterior-posterior boundary in polarized C. elegans embryos. *J Cell Biol* **193**:583-594. doi: 10.1083/jcb.201011094

Hannaford MR, Ramat A, Loyer N, Januschke J. 2018. aPKC-mediated displacement and actomyosin-mediated retention polarize Miranda in Drosophila neuroblasts. *eLife* **7**. doi:10.7554/eLife.29939

Hao Y, Boyd L, Seydoux G. 2005. Stabilization of cell polarity by the C. elegans RING protein PAR-2. *Dev Cell* **10**:199-208. doi: 10.1016/j.devcel.2005.12.015

Hickson GRX, Echard A, O'Farrell PH. 2006. Rho-kinase controls cell shape changes during cytokinesis. *Curr Biol* **16**:359–370. doi:10.1016/j.cub.2005.12.043

Hirata J, Nakagoshi H, Nabeshima Y, Matsuzaki F. 1995. Asymmetric segregation of the homeodomain protein Prospero during Drosophila development. *Nature* **377**:627-30. doi: 10.1038/377627a0

Homem CCF, Knoblich JA. 2012. Drosophila neuroblasts: a model for stem cell biology. *Development* **139**:4297–4310. doi:10.1242/dev.080515

Hurov JB, Watkins JL, Piwnica-Worms H. 2004. Atypical PKC phosphorylates PAR-1 kinases to regulate localization and activity. *Curr Biol* **14**:736-741. doi: 10.1016/j.cub.2004.04.007

Ikeshima-Kataoka H, Skeath JB, Nabeshima Y, Doe CQ, Matsuzaki F. 1997. Miranda directs Prospero to a daughter cell during Drosophila asymmetric divisions. *Nature* **390**:625-629. doi:10.1038/37641

Illukkumbura R, Bland T, Goehring NW. 2019. Patterning and polarization of cells by intracellular flows. *Curr Opin Cell Biol* **62**:123–134. doi:10.1016/j.ceb.2019.10.005

Joberty G, Petersen C, Gao L, Macara IG. 2000. The cell-polarity protein Par6 links Par3 and atypical protein kinase C to Cdc42. *Nat Cell Biol* **2**:531–539. doi:10.1038/35019573

Kemphues KJ, Priess JR, Morton DG, Cheng NS. 1988. Identification of genes required for cytoplasmic localization in early C. elegans embryos. *Cell* **52**:311-320. doi: 10.1016/s0092-8674(88)80024-2

Knoblich JA, Jan LY, Jan YN. 1995. Asymmetric segregation of Numb and Prospero during cell division. *Nature* **377**:624-627. doi:10.1038/377624a0

Knoblich JA. 2010. Asymmetric cell division: recent developments and their implications for tumour biology. *Nat Rev Mol Cell Biol* **11**:849–860. doi:10.1038/nrm3010

Koe CT, Tan YS, Lönnfors M, Hur SK, Low CSL, Zhang Y, Kanchanawong P, Bankaitis VA, Wang H. 2018. Vibrator and PI4KIIIα govern neuroblast polarity by anchoring non-muscle myosin II. *eLife* **7**. doi:10.7554/eLife.33555

Kono K, Yoshiura S, Fujita I, Okada Y, Shitamukai A, Shibata T, Matsuzaki F. 2019. Reconstruction of Par-dependent polarity in apolar cells reveals a dynamic process of cortical polarization. *eLife* **8**. doi:10.7554/eLife.45559

Kuchinke U, Grawe F, Knust E. 1998. Control of spindle orientation in Drosophila by the Par-3-related PDZ-domain protein Bazooka. *Curr Biol* **8**:1357-1365. doi: 10.1016/s0960-9822(98)00016-5

LaFoya B, Prehoda KE. 2021. Actin-dependent membrane polarization reveals the mechanical nature of the neuroblast polarity cycle. *Cell Rep* **35**:109146. doi: 10.1016/j.celrep.2021.109146

Lang CF, Munro E. 2017. The PAR proteins: from molecular circuits to dynamic self-stabilizing cell polarity. *Dev Camb Engl* **144**:3405–3416. doi:10.1242/dev.139063

Laufer JS, Bazzicalupo P, Wood WB. 1980. Segregation of Developmental Potential in Early Embryos of Caenorhabditis elegans. *Cell* **19**:569-577.

Lee CY, Wilkinson BD, Siegrist SE, Wharton RP, Doe CQ. 2006. Brat is a Miranda cargo protein that promotes neuronal differentiation and inhibits neuroblast self-renewal. *Dev Cell* **10**:441-449. doi: 10.1016/j.devcel.2006.01.017

Li L, Vaessin H. 2000. Pan-neural Prospero terminates cell proliferation during Drosophila neurogenesis. *Genes Dev* **14**:147-151.

Mayer M, Depken M, Bois JS, Jülicher F, Grill SW. 2010. Anisotropies in cortical tension reveal the physical basis of polarizing cortical flows. *Nature* **467**:617-621. doi: 10.1038/nature09376

Michaux JB, Robin FB, McFadden WM, Munro EM. 2018. Excitable RhoA dynamics drive pulsed contractions in the early C. elegans embryo. *J Cell Biol* **217**:4230–4252. doi:10.1083/jcb.201806161

Motegi F, Zonies S, Hao Y, Cuenca AA, Griffin E, Seydoux G. 2011. Microtubules induce self-organization of polarized PAR domains in Caenorhabditis elegans zygotes. *Nat Cell Biol* **13**:1361-1367. doi: 10.1038/ncb2354

Munro E, Nance J, Priess JR. 2004. Cortical flows powered by asymmetrical contraction transport PAR proteins to establish and maintain anterior-posterior polarity in the early C. elegans embryo. *Dev Cell* **7**:413–424. doi:10.1016/j.devcel.2004.08.001

Oon CH, Prehoda KE. 2019. Asymmetric recruitment and actin-dependent cortical flows drive the neuroblast polarity cycle. *eLife* **8**. doi:10.7554/eLife.45815

Petronczki M, Knoblich JA. 2001. DmPAR-6 directs epithelial polarity and asymmetric cell division of neuroblasts in *Drosophila. Nat. Cell Biol.* **3**: 43-49.

Prehoda KE. 2009. Polarization of Drosophila neuroblasts during asymmetric division. *Cold Spring Harb Perspect Biol* **1**:a001388. doi:10.1101/cshperspect.a001388

Reymann A-C, Staniscia F, Erzberger A, Salbreux G, Grill SW. 2016. Cortical flow aligns actin filaments to form a furrow. *eLife* **5**. doi:10.7554/eLife.17807

Rhyu MS, Jan LY, Jan YN. 1994. Asymmetric distribution of numb protein during division of the sensory organ precursor cell confers distinct fates to daughter cells. *Cell* **76**:477-491.

Robin FB, McFadden WM, Yao B, Munro EM. 2014. Single-molecule analysis of cell surface dynamics in Caenorhabditis elegans embryos. *Nat Methods* **11**:677-682. doi: 10.1038/nmeth.2928

Rodriguez J, Peglion F, Martin J, Hubatsch L, Reich J, Hirani N, Gubieda AG, Roffey J, Fernandes AR, St Johnston D, Ahringer J, Goehring NW. 2017. aPKC Cycles between Functionally Distinct PAR Protein Assemblies to Drive Cell Polarity. *Dev Cell* **42**:400-415.e9. doi: 10.1016/j.devcel.2017.07.007

Rolls MM, Albertson R, Shih H-P, Lee C-Y, Doe CQ. 2003. Drosophila aPKC regulates cell polarity and cell proliferation in neuroblasts and epithelia. *J Cell Biol* **163**:1089–1098. doi:10.1083/jcb.200306079

Rose L, Gönczy P. 2014. Polarity establishment, asymmetric division and segregation of fate determinants in early C. elegans embryos. *WormBook Online Rev C Elegans Biol* 1–43. doi:10.1895/wormbook.1.30.2

Roth M, Roubinet C, Iffländer N, Ferrand A, Cabernard C. 2015. Asymmetrically dividing Drosophila neuroblasts utilize two spatially and temporally independent cytokinesis pathways. *Nat Commun* **6**:6551. doi:10.1038/ncomms7551

Roubinet C, Tsankova A, Pham TT, Monnard A, Caussinus E, Affolter M, Cabernard C. 2017. Spatio-temporally separated cortical flows and spindle geometry establish physical asymmetry in fly neural stem cells. *Nat Commun* **8**:1383. doi:10.1038/s41467-017-01391-w

Royou A, Sullivan W, Karess R. 2002. Cortical recruitment of nonmuscle myosin II in early syncytial Drosophila embryos: its role in nuclear axial expansion and its regulation by Cdc2 activity. *J Cell Biol* **158**:127–137. doi:10.1083/jcb.200203148

Schober M, Schaefer M, Knoblich JA. 1999. Bazooka recruits Inscuteable to orient asymmetric cell divisions in *Drosophila* neuroblasts. *Nature* **402**: 548-551.

Schuldt AJ, Adams JH, Davidson CM, Micklem DR, Haseloff J, St Johnston D, Brand AH. 1998. Miranda mediates asymmetric protein and RNA localization in the developing nervous system. *Genes Dev* **12**:1847-1857. doi: 10.1101/gad.12.12.1847

Shen CP, Jan LY, Jan YN. 1997. Miranda is required for the asymmetric localization of Prospero during mitosis in Drosophila. *Cell* **90**:449-458. doi: 10.1016/s0092-8674(00)80505-x

Shen CP, Knoblich JA, Chan YM, Jiang MM, Jan LY, Jan YN. 1998. Miranda as a multidomain adapter linking apically localized Inscuteable and basally localized Staufen and Prospero during asymmetric cell division in Drosophila. *Genes Dev* **12**:1837-1846. doi: 10.1101/gad.12.12.1837

Siller KH, Cabernard C, Doe CQ. 2006. The NuMA-related Mud protein binds Pins and regulates spindle orientation in Drosophila neuroblasts. *Nat Cell Biol* **8**:594–600. doi:10.1038/ncb1412

Simões S, Oh Y, Wang MFZ, Fernandez-Gonzalez R, Tepass U. 2017. Myosin II promotes the anisotropic loss of the apical domain during Drosophila neuroblast ingression. *J Cell Biol* **216**:1387–1404. doi:10.1083/jcb.201608038

Smith CA, Lau KM, Rahmani Z, Dho SE, Brothers G, She YM, Berry DM, Bonneil E, Thibault P, Schweisguth F, Le Borgne R, McGlade CJ. 2007. aPKC-mediated phosphorylation regulates asymmetric membrane localization of the cell fate determinant Numb. *EMBO J* **26**:468-80. doi: 10.1038/sj.emboj.7601495

Strome S, Wood WB. 1982. Immunofluorescence visualization of germ-line-specific cytoplasmic granules in embryos, larvae, and adults of *Caenorhabditis elegans*. *Proc Natl Acad Sci* **79**:1558-1562.

Tabuse Y, Izumi Y, Piano F, Kemphues KJ, Miwa J, Ohno S. 1998. Atypical protein kinase C cooperates with PAR-3 to establish embryonic polarity in Caenorhabditis elegans. *Dev Camb Engl* **125**:3607–3614.

Tsankova A, Pham TT, Garcia DS, Otte F, Cabernard C. 2017. Cell Polarity Regulates Biased Myosin Activity and Dynamics during Asymmetric Cell Division via Drosophila Rho Kinase and Protein Kinase N. *Dev Cell* **42**:143-155.e5. doi:10.1016/j.devcel.2017.06.012

Uemura T, Shepherd S, Ackerman L, Jan LY, Jan YN. 1989. *numb*, a Gene Required in Determination of Fate during Sensory Organ Formation in Drosophila Embryos. *Cell* **58**:349-360.

Venkei ZG, Yamashita YM. 2018. Emerging mechanisms of asymmetric stem cell division. *J Cell Biol* **217**:3785-3795. doi:10.1083/jcb.201807037

Wang S-C, Low TYF, Nishimura Y, Gole L, Yu W, Motegi F. 2017. Cortical forces and CDC-42 control clustering of PAR proteins for Caenorhabditis elegans embryonic polarization. *Nat Cell Biol* **19**:988–995. doi:10.1038/ncb3577

Wodarz A, Ramrath A, Grimm A, Knust E. 2000. Drosophila Atypical Protein Kinase C Associates with Bazooka and Controls Polarity of Epithelia and Neuroblasts. *J Cell Biol* **150**:1361–1374. doi:10.1083/jcb.150.6